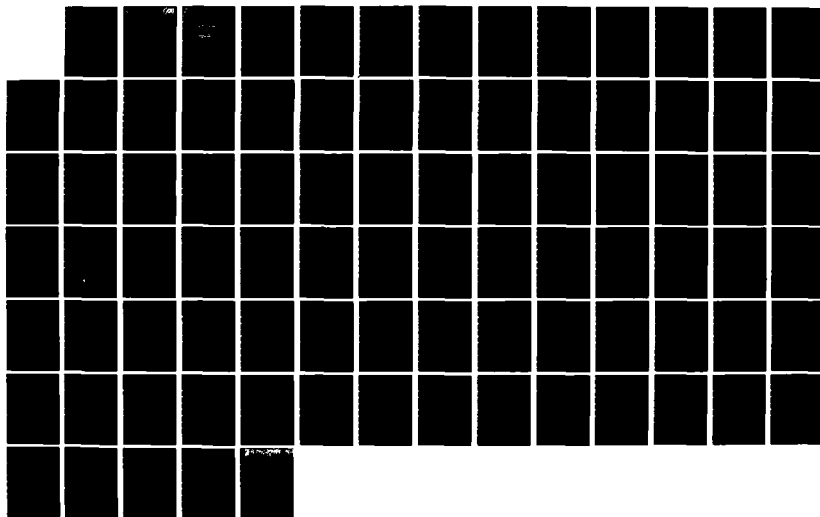
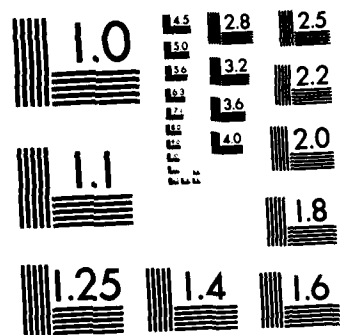


AD-A134 485 LIGHTNING AS A SOURCE OF NO SUB X IN THE TROPOSPHERE 1/1
(U) INSTITUTE FOR DEFENSE ANALYSES ALEXANDRIA VA
M KOWALCZYK ET AL. DEC 81 IDA-P-1590 FAA/EE-82-4
UNCLASSIFIED DTFA01-81-C-10011 F/G 4/1 NL





MICROCOPY RESOLUTION TEST CHART
NATIONAL BUREAU OF STANDARDS-1963-A



U.S. Department
of Transportation
Federal Aviation
Administration



Lightning as a Source of NO_x in the Troposphere

AD-A134485

Office of Environment
and Energy
Washington, D.C. 20591

DTIC
ELECTED
NOV 8 1983
S D D

Marta Kowalczyk and Ernest Bauer

FAA-EE-82-4

DTIC FILE COPY

This document is disseminated under the sponsorship of the Department of Transportation in the interest of information exchange. The United States Government assumes no liability for its contents or use thereof.

The work reported in this document was conducted under Contract No. DT-FAS1-81C-10011 for the Department of Transportation. The publication of this ERA Report does not indicate endorsement by the Department of Transportation, nor should the contents be construed as reflecting the official position of that agency.

Technical Report Documentation Page

1. Report No. FAA-EE-82-4	2. Government Accession No. AD-A134485	3. Recipient's Catalog No.	
4. Title and Subtitle Lightning as a Source of NO_x in the Troposphere		5. Report Date December 1981	
7. Author(s) Marta Kowalczyk and Ernest Bauer		6. Performing Organization Code	
9. Performing Organization Name and Address Institute for Defense Analyses 1801 N. Beauregard Street Alexandria, Virginia 22311		8. Performing Organization Report No. IDA Paper P-1590	
12. Sponsoring Agency Name and Address Department of Transportation Federal Aviation Administration Office of Environment and Energy Washington, D.C. 20591		10. Work Unit No. (TRAIS)	
		11. Contract or Grant No. DT-FA01-81C-10011	
		13. Type of Report and Period Covered Final	
15. Supplementary Notes		14. Sponsoring Agency Code	
16. Abstract The contribution of lightning to the global tropospheric NO _x budget is estimated. The injection height of the NO _x as well as its latitudinal distribution is provided for use in 2-D atmospheric models.			
 Several components of the NO _x production estimate are reviewed in detail. Numerical modeling calculations, experimental simulations, as well as in-situ measurements are examined to determine the efficiency of NO _x production by lightning. Global lightning distributions from satellites are used to derive a mathematical expression for the seasonal and latitudinal lightning rate. Specific attention is given to the latitudinal behavior of the height of NO _x injection and the partitioning of the lightning rate between cloud-to-ground flashes and intracloud discharges. Various mechanisms for the loss of NO _x through rainout during the accompanying thunderstorm are examined and are found to be ineffective. The annual, global NO _x production rate derived here is 5.7×10^{12} gN/yr for all forms of lightning.			
17. Key Words NO _x , lightning, tropospheric inventory, rainout, NO _x source strengths, cloud-to-ground, intracloud, global lightning distribution, 2-D NO _x distribution.	18. Distribution Statement Document is available to the public through the National Technical Information Service, Springfield, VA 22151		
19. Security Classif. (of this report) UNCLASSIFIED	20. Security Classif. (of this page) UNCLASSIFIED	21. No. of Pages 84	22. Price

Accession For	
NTIS GRA&I	<input checked="" type="checkbox"/>
DTIC TAB	<input type="checkbox"/>
Unannounced	<input type="checkbox"/>
Justification	
By	
Distribution/	
Availability Codes	
Dist	Avail and/or Special
A/1	



ABSTRACT

The contribution of lightning to the global tropospheric NO_x budget is estimated. The injection height of the NO_x as well as its latitudinal distribution is provided for use in 2-D atmospheric models.

Several components of the NO_x production estimate are reviewed in detail. Numerical modeling calculations, experimental simulations, as well as in-situ measurements are examined to determine the efficiency of NO_x production by lightning. Global lightning distributions from satellites are used to derive a mathematical expression for the seasonal and latitudinal lightning rate. Specific attention is given to the latitudinal behavior of the height of NO_x injection and the partitioning of the lightning rate between cloud-to-ground flashes and intracloud discharges. Various mechanisms for the loss of NO_x through rainout during the accompanying thunderstorm are examined and are found to be ineffective. The annual, global NO_x production rate derived here is 5.7×10^{12} gN/yr for all forms of lightning.

ACKNOWLEDGEMENTS

Special thanks are due to M. Burns (IDA), R. Fox (IDA), J. Fishman (NASA-Langley), H.S. Johnston (University of California, Berkeley), R.C. Oliver (IDA), and R.E. Orville (SUNY Albany) for their timely review of this document; to B. Edgar (Aerospace Corp.) and M. Kotaki (Radio Research Labs., Japan) for providing us with preprints and limited-distribution reports of the lightning-counting experiments; and to A. Aikin (NASA Goddard) for many helpful discussions.

TABLE OF CONTENTS

Abstract	iii
EXECUTIVE SUMMARY	S-1
A. Introduction	S-1
B. NO _x Production by Lightning	S-2
C. Global Distribution of NO _x from Lightning	S-3
D. Intracloud NO _x Production Efficiency	S-4
E. Injection Height and Residence Time	S-4
F. Internal Rainout	S-4
G. Data for 2-D Model	S-5
H. Recommendations	S-7
I. INTRODUCTION	1
II. NO_x PRODUCTION BY LIGHTNING	7
A. Numerical Model Calculations	7
1. A Description of Lightning Models	7
2. Freeze-out Temperatures	9
3. Model Comparison	10
B. Experimental Simulations with Laboratory Discharges	11
1. Low Energy Discharges	11
2. High Energy Discharges	11
C. Production by Lightning: NO _x /Flash	12
1. Previous Estimates	12
2. In-Situ NO _x Measurements	13
D. Previous Estimates for Global NO _x	16
III. GLOBAL DISTRIBUTION OF LIGHTNING AND NO_x	19
A. Global Lightning	19
1. Local Flash Rate	19
2. Intracloud vs Cloud-to-Ground Lightning	20
3. Global Distribution of Lightning	25
4. Globally Integrated Lightning Rate	32
B. Injection Height of NO _x	35
C. Recommended Treatment of Lightning and NO _x Distributions	40

IV. RAINOUT OF NO_x PRODUCED BY LIGHTNING	43
A. NO_x Loss	45
1. NO _x Loss: HNO ₃ Formation in High Local NO _x Air	45
2. NO _x Loss: HNO ₃ Formation by NO ₂ + OH + M	48
3. NO _x Loss: HNO ₃ Formation via N ₂ O ₅	51
4. NO _x Loss: Dry Deposition	53
5. NO _x Loss: Aerosol Scavenging and Rainout	53
B. HNO₃ Loss: Rainout, Dry Deposition and Heterogeneous Scavenging	55
V. UNCERTAINTIES AND RECOMMENDATIONS	59
A. Uncertainties	59
B. Recommendations	60
Reference List	63

LIST OF TABLES

S-1. Source Strengths of Tropospheric NO _x	S-2
S-2. Annual NO _x Injection Rate from Lightning: 2-D Distribution	S-6
1. Number of Strokes Within a Flash	3
2. Previous Theoretical and Experimental Estimates of NO _x Production By Lightning	8
3. NO ₂ Produced by Lightning	15
4. Summary of Lightning Flash Data Used for Global NO _x Estimates	17
5. Radio Frequency Emission from Cloud and Ground Strokes	21
6. Strengths and Weaknesses of the Primary Data Sets	28
7. Lightning Flash Rate, Latitudinal and Seasonal Distribution	31
8. Lightning Flashes Counted by Satellite	33
9. Some Representative Heights of Cloud Discharges	36
10. Summary of Lightning Parameters and NO _x Injection Rate	39
11. Approximate Lifetime for Individual NO ₂ Loss Mechanisms	44
12. Equilibrium of HNO ₃ with Water	56
13. HNO ₃ Scavenging by Clouds and Rainfall	56

LIST OF FIGURES

1. Relation between observed values of the ratio, N_c/N_g of cloud flashes to ground flashes and latitude, λ . The 29 data points and the empirical relation $N_c/N_g = 4.16 + 2.16 \cos 3\lambda$ are shown. 23
2. Optical observation of lightning rate from DMSP satellite for dusk in April. 26
3. Lightning rate data from the HF radio noise data obtained by the ISS-b satellite for spring in the late afternoon and evening. 26
4. Global distribution of atmospheric radio noise obtained from ground monitoring stations. Spring season, 1200-1600 hours. 27
5. Springtime global distributions determined from ground-based observations of thunderstorms. 27
6. Latitudinal and seasonal dependence of the lightning rate observed from the DMSP satellite. The curve shown for the dusk data was calculated by equation 3.6. 29
7. 2-D NO_x distribution in 10^{12} gN/yr injected into the troposphere by lightning. 42
8. Diurnal behavior of the NO_x and HO_x chemical systems in the troposphere at 15° N latitude equinox, calculated with 1-D model. The upper set of figures is for ground level conditions; the lower set is for an altitude of 6 km. 47
9. Curve A, Data for $O_3 + h\nu \longrightarrow O(^1D) + O_2$ photo-dissociation constant, showing the effect of passing clouds. \square was calculated using atmospheric absorption and Rayleigh scattering. Curve B is $\exp(-1/\cos \theta)$. 49

EXECUTIVE SUMMARY

A. INTRODUCTION

This paper was prepared for the Federal Aviation Administration, High Altitude Pollution Program as a part of the contracted task, Analysis of Aircraft Effects: Natural Atmospheric Perturbation.

Present and projected transport aircraft operations will inject a substantial amount of oxides of nitrogen ($\text{NO}_x = \text{NO} + \text{NO}_2$) into the atmosphere at cruise altitudes. The significance of these injections on atmospheric ozone and overall atmospheric chemistry can only be determined by comparing the aircraft source with all other sources, natural and anthropogenic. A comparison of the NO_x source strengths shown in Table S-1 indicates that lightning is a significant natural source of tropospheric NO_x . This paper quantifies the injection rate of NO_x due to lightning and its variation with altitude, geographic location, and season, pointing out significant uncertainties in the estimates.

A global lightning rate of 300 flashes/s has been adopted here, consisting of approximately 20 percent cloud-to-ground flashes and 80 percent intracloud discharges. A production rate of $10^{26} \text{ NO}_x/\text{flash}$ for ground flashes (Noxon 1976; 1978), and $10^{25} \text{ NO}_x/\text{flash}$ for cloud discharges yields an annual global production rate of 5.7 Tg N/yr (1 Tg = 10^{12} grams) from lightning with an estimated uncertainty range of 2-20 Tg N/yr.

The discussion begins with a description of four forms of atmospheric electricity related to lightning, listed here in the order of their energy dissipation per unit length; corona discharges, intracloud discharges, cloud-to-ground strokes and,

superbolt flashes. The net NO_x production by electrical discharges is proportional to the discharge energy. Corona discharges, the low-energy discharges which can occur almost continuously during a thunderstorm, actually contribute only minimally to the NO_x production. At the other extreme, superbolt flashes are extremely energetic but rare, so that their cumulative NO_x production rate is also minimal. The rest of the report concerns itself with the NO_x production from intracloud discharges and cloud-to-ground flashes.

TABLE S-1. SOURCE STRENGTHS OF TROPOSPHERIC NO_x *

Tg N/yr

Natural Sources:

Lightning	5.7
Forest Fires	1.7
Transport from Stratosphere	0.5
Cosmic rays	0.06
Exhalation from soils	10

Anthropogenic Sources (1975 Estimates):

Fossil fuel combustion	20
Biomass burning**	3.3
Aircraft	0.15
NH ₃ decomposition (also natural)	<8

*Compiled from Bauer (1982);

**Includes deforestation due to population increase, shifting agriculture, and the burning of firewood, bush, and savannah.

B. NO_x PRODUCTION BY LIGHTNING

The amount of NO_x produced by lightning has been measured in-situ, simulated in the laboratory with spark discharges, and numerically modeled by various methods. Most of the final estimates are between $(0.6-4) \times 10^{26}$ NO_x molecules produced per lightning flash.

This study adopts the recommendation from three in-situ measurements by Noxon (1976, 1978). Under the dark sky conditions during a thunderstorm the NO produced by lightning is largely converted to NO₂; in this study NO₂ is assumed to be equivalent to NO_x. Noxon recorded the absorption spectrum of

the overhead column of NO_2 before, during, and after a thunder-storm. Noxon's (1976) first measurement of $10^{26} \text{ NO}_2/\text{flash}$ was supported by two subsequent experiments (Noxon 1978), and is in reasonable agreement with most of the numerical model simulations of lightning in air. In-situ measurements such as Noxon's have several advantages for an inventory. First, the lightning process is genuine; therefore, assumptions about lightning parameters such as energy deposited per stroke and additional NO_x produced by subsequent strokes in a flash need not be made. Second, the problem of rainout immediately after the flash need not be considered, because the in-situ measurements give a net NO_x production.

C. GLOBAL DISTRIBUTION OF NO_x FROM LIGHTNING

In this work, global distributions of lightning obtained from the DMSP and ISS-b satellites* have been emphasized, although in general, an excellent qualitative agreement exists with the historical distribution of thunderstorms. It should be noted that the ISS-b satellite measurement by Kotaki et al. (1981) was done by sensing the radio-frequency emissions from lightning discharges, which is an experimental method sensitive to both cloud-to-ground flashes and intracloud discharges, whereas the DMSP satellite measurement by Turman and Edgar (1980) was done with an optical sensor, a method which may discriminate against the less energetic intracloud discharges.

The globally integrated rate of lightning obtained from these two measurements differ by a factor of three, i.e., DMSP = 80 ± 40 flashes/s and ISS-b = 280 flashes/s. The discrepancy between these two determinations may be due to the normalization required to convert the DMSP satellite data to an absolute lightning flash rate. Specifics about the normalization are discussed in the main text.

*DMSP = Defense Meteorological Satellite Program, USA
ISS-b = Ionospheric Sounding Satellite, Japan.

D. INTRACLOUD NO_X PRODUCTION EFFICIENCY

The efficiency of NO_X formed by lightning, as well as its altitude of injection in the atmosphere, differs for cloud discharges and ground strokes. In this work, NO_X production by intracloud discharges was assumed to be one-tenth as efficient when compared to a ground flash, based on experimental evidence that the amount of NO_X produced is proportional to the discharge energy. This assumption is a major source of uncertainty, since no direct experimental verification of the energy deposited by intracloud discharges exists.

E. INJECTION HEIGHT AND RESIDENCE TIME

The altitude of NO_X production is not the altitude of NO_X injection because of the violent updrafts and downdrafts associated with the center of a thunderstorm. The stabilization height was taken to be directly below the local tropopause, that is, 12 km for midlatitudes and 15 km for the tropics. A density-weighted vertical distribution was proposed for the NO_X injected by both intracloud and cloud-to-ground lightning. Experimental evidence in which the luminosity of the lightning channel decreased with height and the tendency to produce a density-weighted vertical distribution with sufficient atmospheric mixing support this assumption. The NO_X from intracloud discharges was assumed to be distributed in a 5-km band below the local tropopause and the NO_X from ground flashes was distributed uniformly between that level and the ground.

The effect of chemical injections on atmospheric photochemistry depends on the residence time of the chemical species, which, in turn, depends on the altitude and latitude of the injection. NO_X injected at high tropospheric altitudes, especially near the tropopause, will remain in the atmosphere significantly longer than an equal amount from a source near the ground. Similarly, the residence time of NO_X in regions where the net flow

in atmospheric circulation is upwards, as in the tropics, will be longer than in regions of net downward flow.

F. INTERNAL RAINOUT

Various mechanisms for NO_x loss at ambient temperatures were examined and were found to be inefficient on a time scale comparable to the lifetime of a thunderstorm. The NO_2 production estimate from Noxon's (1976; 1978) in-situ measurements can be considered to be the residual NO_2 which remains after any initial rainout of HNO_3 or HNO_2 formed in the hot lightning channel. Any losses during the thunderstorm that occur after Noxon's measurements represent true losses to the inventory but, as mentioned previously, these losses were found to be small.

G. DATA FOR 2-D MODEL

The recommended treatment for the 2-D distribution is summarized here. An annual average lightning rate of 300 flashes/s, including both intracloud discharges and cloud-to-ground flashes, was chosen. This rate was partitioned among the latitudes and months of the year according to the global lightning distributions observed by Turman and Edgar (1980) from the DMSP satellite.

The monthly values can be appropriately averaged for seasonal or annual calculations. The values at each latitude were in turn partitioned between ground flashes and intracloud discharges based on the recommendations of Prentice and Mackerras (1977). The upper bound of the intracloud injection region is defined by the local tropopause. For use in a numerical model, the NO_x production rate in each injection region must be distributed among the number of altitude bins available in the model. A density-weighted distribution is recommended. Table S-2 specifies the annual NO_x injection rate in Tg N/yr as a function of latitude and altitude.

Several uncertainties can be identified in the estimate of the lightning contribution to the global NO_x budget in the

TABLE S-2. ANNUAL NO_x INJECTION RATE FROM
LIGHTNING: 2-D DISTRIBUTION

ALTITUDE km	10 ¹² gN/yr-km*						Atmospheric Number Density** x 10 ³³ km ⁻³				
	-60	-50	-40	-30	-20	-10	0	10	20		
15					0.020	0.039	0.049	0.045	0.033	0.030	4.4
14					0.024	0.046	0.057	0.057	0.039	0.035	5.1
13					0.027	0.052	0.066	0.060	0.045	0.041	6.0
12	—	0.001	0.006		0.032	0.062	0.079	0.072	0.053	0.049	7.0
11	—	0.002	0.007		0.036	0.071	0.089	0.081	0.060	0.055	8.1
10	—	0.002	0.008		0.016	0.028	0.031	0.030	0.024	0.024	9.1
9	—	0.002	0.009		0.018	0.031	0.035	0.034	0.027	0.027	10.3
8	—	0.003	0.010		0.021	0.035	0.040	0.038	0.031	0.030	11.6
7	—	0.003	0.011		0.023	0.039	0.044	0.043	0.034	0.034	13.0
6	—	0.003	0.013		0.026	0.044	0.049	0.048	0.038	0.038	14.5
5	—	0.004	0.014		0.029	0.049	0.055	0.053	0.043	0.042	16.2
4	—	0.004	0.015		0.032	0.054	0.061	0.059	0.048	0.046	18.0
3	—	0.005	0.017		0.035	0.060	0.068	0.065	0.053	0.051	19.9
2	—	0.005	0.019		0.039	0.066	0.075	0.072	0.058	0.057	22.0
1	—	0.006	0.021		0.042	0.073	0.083	0.079	0.064	0.063	24.3
0											
	LATITUDE										

*The zonal areas within 10-degree latitude intervals are given in Table 10 to facilitate conversion to injection units such as molecules/cm³s.

** U.S. Standard Atmosphere, 1976.

troposphere:

- (1) The NO_x production efficiency for intracloud discharges
- (2) The NO_x production efficiency in the tropics
- (3) The injection height of NO_x produced during a lightning storm both at midlatitudes and in the tropics
- (4) The normalization of the global lightning rate measured by satellites, especially in the tropics.
- (5) The ratio of cloud discharges to ground flashes, also with particular emphasis in the tropics where current data is scarce.

The accumulated uncertainty for the measured quantities has been estimated to be within one order of magnitude. It is not possible to estimate the uncertainty for the unmeasured quantities such as the NO_x production efficiency by intracloud discharges and the injection height.

H. RECOMMENDATIONS

Several experiments that could eliminate most of the uncertainty in the lightning-generated NO_x estimate are recommended. In most cases, these can be carried out with currently developed equipment and some minor modifications.

- (1) The F-106B aircraft used in the NASA-Langley Storm Hazards Project, which is currently equipped to fly within thunderstorms, should be fitted to measure NO_x at various altitudes within the storm cloud, at the perimeter of the cloud, and outside the cloud. This would answer the questions concerning NO_x production efficiency as well as those concerning the height of injection in the region of net updraft in the center of the thundercloud and in the region of net downdraft at the perimeter. Continued measurements as the storm passes would indicate the rate of NO_x dissipation and chemical removal.

- (2) The tropical regions should be included if any further experiments of the NO_x production efficiency by lightning, such as Noxon's column measurements, are done.
- (3) The calibration of lightning flash rate measured by satellites needs more serious consideration. The several global maps generated by satellite have similar distributions, but a consensus for the globally averaged value does not exist. Any ground-based calibration data must include tropical as well as mid-latitude measurements. Attention must also be given to the ratio of intracloud discharges to ground flashes, Nc/Ng for the calibration points chosen.
- (4) The uncertainty in the ratio of the number of intracloud discharges/ground flashes, Nc/Ng , for tropical regions needs to be reduced by additional measurements. It is emphasized that most lightning occurs in the tropics but current measurements are concentrated in the mid-latitudes.

I. INTRODUCTION

To understand the significance of anthropogenic NO_x emissions, the magnitude and altitude of the emissions must be compared to natural sources within the atmosphere. The contribution of lightning has, to date, been a major uncertainty in such a global NO_x source inventory. Current estimates of the NO_x production rate by lightning vary by a factor of 50 from 1.8 to 90 Tg N/yr. This range, however, is not indicative of the uncertainty of global NO_x production by lightning since not all the estimates were made with the same initial conditions and assumptions about the lightning process. If only cloud-to-ground flashes are counted, the estimates are between 1.8 and 22 Tg/yr and if intracloud lightning is included, the range becomes 9 to 90 Tg/yr. A comparison with anthropogenic combustion sources, estimated at about 20 Tg N/yr (Crutzen 1979), shows that these estimates span the entire range from a minor to a significant source of NO_x . This paper examines the separate components necessary to make an estimate of the global production rate of NO_x by lightning. Previous work in which global NO_x production rates were estimated are examined, with particular emphasis on the experimental and theoretical basis of previous estimates. Recommendations are made based on the least ambiguous data source. The remainder of this chapter will discuss some basic information about the lightning process and other forms of atmospheric electricity that may be sources of NO_x in the troposphere.

It is clear to anyone who has seen the damage to an object struck by lightning that massive energies are released. During a storm, large potential energies are created when regions of

positive and negative charge accumulate within a cloud. The exact mechanism of the charge generation, separation, and accumulation is unknown, but most theories consider the process to be due either to the frictional effects of falling water and ice particles within a cloud or to the transport and accumulation of external charge by convective circulation within the cloud. When sufficient charge has accumulated, on the order of hundreds of coulombs within a thundercloud a few kilometers wide, the high electric field and space-charge effects can result in a point, or corona, discharge. An arc discharge is created if a sufficient potential difference exists between the cloud and the far edge of the corona discharge. A portion of the cloud's charge can then be transferred to the leading point of the newly created ionized path. The process can be repeated in a stepwise manner so that an atmospheric breakdown path many kilometers long can result, even though a direct one-step breakdown would not be possible. The partially ionized breakdown channel is called the stepped leader.

A potential for massive charge neutralization exists if the stepped leader reaches the ground. The neutralization that begins at the ground and then progresses up the stepped leader path is referred to as the return stroke. About 90 percent of the lightning stroke energy is dissipated in the return stroke, but only a fraction of the cloud's total charge is neutralized. Subsequent strokes along the same lightning channel can neutralize the residual charge.

A typical number of strokes per lightning flash is three to four; however, the number depends on factors such as lightning type, storm type, and specific geographic location. A clear dependence on latitude is not evident. The stroke-per-flash data summarized in Table 1 shows that multiple strokes are prevalent in New Mexico and single flashes are more common on Mount San Salvatore, Switzerland. Schonland (1956) reported that 50 percent of the flashes out of a total of 1800 in South

Africa had four or more strokes per flash. He also noted that multiple strokes occur more readily in large frontal storms than in small convective storms.

TABLE 1. NUMBER OF STROKES WITHIN A FLASH

Number of Strokes per Flash	Percentage of Total Flashes		
	South Africa ^a	New Mexico ^b	Switzerland ^c
1	13	12.2	76.5
2	19	26.5	7.7
3	18	7.3	4.8
4	20	4.9	1.9
5	12	-	2.3
6		14.6	1.4
7	18	2.5	1.0
8		4.9	0.7
>8		27.1	3.8
Total Number of flashes	530	41	1026
Mean value: strokes/flash	$1220/530=2.3$	$265/41=6.5$	$1950/1026=1.9$

^a Malan (1956), cited in Berger (1977).
^b Kitagawa et al. (1962), cited in Berger (1977).
^c Berger (1972), cited in Berger (1977).

An intracloud discharge can occur if a leader within a cloud, called a streamer, reaches a point with a significantly lower potential, i.e., a differently charged portion within the same cloud, or to another cloud. The current of an intracloud discharge, about 100 amperes, is significantly less than the 10^4 to 10^5 amperes characteristic of the cloud-to-ground return stroke. It should be noted that cloud-to-ground lightning generally has an intracloud component but not all intracloud lightning eventually hits the ground.

Most corona discharges do not develop into cloud-to-ground lightning or intracloud and intercloud discharges. Typically, the energy dissipated by a corona discharge is low, with currents on the order of microamperes. Berger (1977) cites an example of an experiment on San Salvatore where corona discharges transported a total of 72 coulombs to the experimental tower within 20 hours. This is comparable to the charge transfer within a single lightning stroke. It must be noted that the corona discharge process occurs continuously over a large surface area, therefore the time and space integrated charge transfer can be quite large. For example, the charge transferred from the clouds to the ground by corona discharges has been estimated from an integration of current records and was found to be on the average 20 times greater than the charge transferred by cloud-to-ground lightning strokes (Latham and Stromberg 1977). Even weak electrical discharges can cause molecular dissociation and recombination, as is evident from experimental discharges in primitive atmospheres in which amino acids are synthesized over long periods of time.

Routine satellite coverage of the earth has revealed the existence of a rare type of lightning called a superbolt flash in which the energy dissipated is over 100 times more powerful than typical lightning (Turman 1977). For over 5 years the sensors aboard the Vela V satellites recorded an average of 5 superbolt flashes/year with powers greater than about 3×10^{12} watts (Turman 1979). This low lightning rate is insufficient to affect the global NO_x production, however it may cause local enhancement near Japan where most superbolts occur. The existence of superbolts bring out a crucial but unanswered question; are the superbolts a separate physical phenomenon, or are they the high-energy part of an energy distribution of lightning? If the former is true, the superbolts have a negligible effect on the annual NO_x production by lightning. If the latter is true, then the wide energy distribution

makes it more difficult to reach conclusions about a "typical" lightning flash. In this case one must be careful to work with an adequate statistical sample.

NO_x ($\text{NO}_x = \text{NO} + \text{NO}_2$) production can occur for most types of atmospheric discharges; the amount of NO_x production depends on the discharge energy and the duration of the discharge. To date, the studies of NO_x production by lightning have concentrated on the cloud-to-ground lightning stroke. On energetic grounds alone this approach may be justified, since the powerful return stroke of cloud-to-ground lightning releases the most energy and produces the most NO_x per unit distance. Experimental discharge studies, discussed in Chapter II, indicate that the NO_x yield per joule is approximately constant for low and high energy discharges between 10 and 10^6 J/m, which implies that the NO_x produced is directly proportional to the discharge energy. Although corona discharges occur continuously during a lightning storm the discharge energy is quite small. Measurements by Noxon (1978) indicate that corona discharges are inefficient at NO_x production. The measured NO_2 concentrations during corona activity were not too different from typical ambient values.

In order to appreciate the magnitude of NO_x production contributed by each type of discharge, it is necessary to consider the cumulative effects, discharge times, distances, and frequencies. Although intracloud discharges contain no large energy sink like the return stroke they can travel over longer distances. Intercloud strokes in excess of 50 kilometers have been recorded. It is also necessary to consider the frequency of discharge events. Intracloud discharges occur up to six times as often as cloud-to-ground strokes and, as mentioned previously, corona discharges occur almost continuously during a thunderstorm. This will be considered in more detail in Chapter 3 when lightning counting is discussed. Several books have been written recently about the basic properties of

lightning; for more detail the reader is referred to them (Uman 1969; Chalmers 1967; Golde 1977).

II. NO_x PRODUCTION BY LIGHTNING

Estimates of the amount of NO_x produced per unit energy by a lightning stroke have been obtained by numerical simulation with various model approaches, laboratory simulations with spark discharges in air, and in one case with an in-situ measurement of NO₂ in a lightning storm. Table 2 shows that the range of these estimates span an order of magnitude. This section will briefly discuss the techniques used to estimate NO_x production specifically addressing the variability evident in Table 2.

A. NUMERICAL MODEL CALCULATIONS

1. A Description of Lightning Models

NO production by lightning is modelled by two different approaches: the shock heating model proposed by Tuck (1976) and extended by Chameides et al. (1977) and Chameides (1979a, 1979b) and the hot channel model proposed by Hill et al. (1980). Both models calculate NO_x production by the number of NO molecules produced in air at high temperatures which are then frozen in as the air expands and cools. The two models differ in the mechanism that produces the heating. A comparison of the two models and an evaluation of NO yields is given by Hill (1979b).

The shock heating model is based on the shock wave theory of Lin (1954). The model assumes an infinitely narrow line source for lightning and an instantaneous release of energy which creates a sharp pressure discontinuity. Heating occurs as the shock wave that is created propagates radially from the lightning sources region. It is this heating that causes the molecular dissociation and eventual recombination to form NO.

TABLE 2. PREVIOUS THEORETICAL AND EXPERIMENTAL ESTIMATES OF NO_x PRODUCTION BY LIGHTNING

Lightning Model	NO _x Produced			References
	NO _x /J 10 ¹⁶ molec/J	NO _x /flash 10 ²⁵ molec/ flash	Global NO _x 10 ¹² gN/yr	
Shock wave	4	2.5 1.1	6	Tuck 1976
Experimental observation	-	10	-	Noxon 1976
Hot channel	6	32-40	-	Griffing 1977
Shock wave	3-7	6-14	30-40	Chameides et al. 1977
Experimental spark simulation*	6+1(10)* 8+2(1350)*	-	-	Chameides et al. 1977
Shock wave	8-17	16-34	35-90	Chameides 1979
Hot channel	80	6	4.5	Hill 1980
Review	-	0.6	3	Dawson 1980
Experimental spark simulation*	5+2(10 ⁵)*	0.5	1.8+0.7	Levine et al. 1981
Review	3.7	0.74	2.1	Hameed et al. 1981

*The discharge energy in J/m is listed in parentheses for the experimental spark simulations.

The channel heating model is based on theories of intense localized sources of ohmic heat in the atmosphere (Brode 1955; Hill 1971; Ploooster 1971). Lightning is simulated by a time-dependent stroke which heats a channel of air a few centimeters wide as it propagates. The molecular heating is caused directly by the lightning stroke. At first the extreme temperatures and high electron densities cause rapid molecular dissociation, excitation, and ionization but as the hot air expands and cools, the ions and molecules recombine.

2. Freeze-Out Temperatures

Both mechanisms result in heated air that, presumably, can cause the massive dissociation and ionization of atmospheric species that has been observed experimentally from emission and absorption lines (Salanave et al. 1962; Salanave 1969; Wallace 1960; Orville 1967, 1968). Early in the lifetime of the lightning stroke, radiative emission, collisional deexcitation and ionic recombinations neutralize the plasma. When the temperature has dropped to about 4000 K, neutral recombination reactions to form NO can proceed rapidly. If the cooling rates are sufficiently slow, chemical equilibrium can exist for the production and destruction of NO. When the air has cooled further, to the range between 2000-3000 K, the actual NO concentration will not fall as fast as the equilibrium concentration. Beyond this point the NO formed at higher temperatures is no longer efficiently destroyed and it remains in the air at the concentration characteristic of the freeze-out temperature (Gilmore 1974, 1975). Volume mixing ratios of a few percent NO in equilibrium air can result.

The precise amount of NO produced is very sensitive to the freeze-out temperature which in turn depends on the cooling rate of the lightning channel gases. Faster cooling rates result in higher freeze-out temperatures. The simulations of the shock wave and hot channel models for similar lightning initial conditions show that the shock wave travels faster than

the heated gases in the hot channel. Therefore, for the shock model calculations one would expect a faster cooling rate for the gases at the shock front and a higher freeze-out temperature. Model calculations with identical initial conditions indicate freeze-out at 3000 K for the hot channel model and 4000 K for the shock heating model (Hill et al. 1980), confirming this expectation.

3. Model Comparison

The difference between the lightning models becomes most evident when one compares the volume of air that has been raised to the freeze-out temperature. As mentioned previously, model calculations by Hill et al. (1980) predict that early in the lifetime of the lightning channel, the shock wave propagates faster and soon decouples from the hot gases in the original lightning channel. This has recently been confirmed by a set of time-dependent Schlieren photographs of discharges in air (Picone et al. 1981). The experiments show that a separation of the shock wave from the hot channel has occurred 8 microseconds after the initiation of the discharge, and that at 100 microseconds the shock wave radius had quadrupled, whereas the hot channel remained approximately the same size. Calculations using both models with identical initial conditions were done to determine the propagation radius at the freeze-out temperature (Hill et al. 1980). For the hot channel model an outer radius of 16 cm was calculated, with freeze-out occurring at 3000 K. The shock wavefront in the shock heating model had travelled 1.6 cm before freeze-out at 4000 K. The smaller volume of air calculated by the shock heating model is partially offset by a greater air density. The shock wavefront envelops air with ambient density, whereas the hot air density within the hot channel near the freeze-out temperature is approximately one tenth ambient (i.e., 300 vs. 3000 K). As a result of these considerations alone, the NO yield estimates per joule discharge energy for the shock heating model are at least a factor of five and perhaps ten less than the hot channel estimates.

B. EXPERIMENTAL SIMULATIONS WITH LABORATORY DISCHARGES

Experimental determinations of the amount of NO_x produced per joule discharge energy have been studied in both the high and low discharge energy regimes. Chameides (1979) pointed out that it is possible that results from low-energy discharges may underestimate the NO_x production by lightning. An examination of three discharge experiments over the energy regime below 10^5 J/m , as well as various studies of nuclear explosions, indicates an energy-dependent trend for the NO production efficiency which was reproduced by a shock model calculation (Chameides 1979). The validity of this trend needs to be verified by an experimental determination at higher energies other than nuclear explosions since it is not clear that the mechanism and time scales of nuclear explosions and linear discharges are comparable. At lower energies, the experimental uncertainty is large enough to make conclusions about a trend uncertain.

1. Low-Energy Discharges

Lightning parameters have been studied with a variety of experimental techniques in an extensive set of experiments on the Westinghouse 4-meter spark chamber (Krider et al. 1968; Dawson et al. 1968; Uman et al. 1968, 1970). These experiments have been discussed in detail in a recent review (Dawson 1980) and will not be repeated here. Experimental spark simulations by Chameides et al. (1977) with low and medium energy deposition resulted in similar NO_x/J yields within the limits of uncertainty. Table 2 shows that these results are also similar to theoretical values calculated with the shock model approach.

2. High-Energy Discharges

An experimental laboratory discharge capable of generating between 10^5 and 10^6 J/m discharge energy was used by Levine et al. (1981) to simulate lightning. Their simultaneous measurements of $\text{NO}_x = \text{NO} + \text{NO}_2$, NO and O_3 showed that initially only NO was produced by the discharge. Chemical conversion to NO_2 by $\text{NO} + \text{O}_3 \rightarrow \text{NO}_2 + \text{O}_2$ which follows rapidly in air must occur

with ambient O_3 since no enhancement in O_3 concentration was observed after the discharge. The value obtained for the NO_x production per joule discharge energy at high energies is in line with previous experimental results at lower energies.

C. PRODUCTION BY LIGHTNING: NO_x /FLASH

1. Previous Estimates

Inherent in most estimates of the amount of NO_x produced in a lightning stroke is the energy of a typical lightning stroke in J/m , the length of an average lightning stroke, and the additional NO_x produced by subsequent strokes within a flash. These lightning parameters (listed in Table 4 on page 17), rather than the chemical production factors, are the largest sources of variability in the previous estimates of NO_x production.

Until very recently, a value of $10^5 J/m$ has been adopted for the energy deposited by a lightning stroke, based on the recommendations of Chalmers (1967) and Uman (1969). A recent review by Hill (1979a) extensively discussed and reevaluated previous electrical, optical, and acoustic measurements of energy dissipation. The new recommendation of $10^4 J/m$, which is an order of magnitude less, causes the NO_x production per stroke estimated by Hill et al. (1980) to also be an order of magnitude lower.

Values suggested for the average stroke length vary between 5 and 10 km. Lightning channel lengths are typically longer than 5 km for tropical thunderstorms where most lightning activity occurs.

Another parameter that needs to be estimated, but for which no direct experimental evidence exists, is the amount of additional NO_x produced by subsequent lightning strokes beyond the first one. Chameides et al. (1977) and Chameides (1979) consider an average of four strokes per flash and count each one as a separate event. Most probably this will overestimate the NO_x produced. The quantity that needs to be considered is

the increase of heated air in the lightning channel caused by the subsequent strokes within the flash. Hill et al. (1980) assumes that the amount of energy deposited to the lightning channel is proportional to the charge deposited by each individual stroke and that the first stroke is about five times as energetic as the subsequent strokes. For a three-stroke flash, Hill et al. (1980) obtains heated air for the entire flash that is 1.5 ± 0.5 times the amount for a single stroke. Dawson (1980) favors even a lower estimate. He argues that the first stroke is by far the most energetic and that all strokes within a flash occur along the identical channel with insufficient time between strokes for diffusive losses of NO_x . His review recommends counting first strokes only. Direct experimental verification is needed; however, some insight may be obtained from a set of low-energy discharge experiments by Chameides et al. (1977). The rate of sparking through air was varied between 8 and 53 per minute. The concentration of the NO_x produced was proportional to the total energy deposited; a separate dependence on the sparking rate was not observed. This result tentatively confirms the lower estimates for additional NO_x produced within multiple-stroke flashes but it needs to be verified at higher energies and at higher sparking frequencies to properly simulate the multiple-stroke case for lightning.

2. In-Situ NO_x Measurements

The only direct measurements of gas phase NO_x produced by lightning are the spectroscopic determinations by Noxon (1976; 1978). Tropospheric measurements were obtained from the ground by observing spectra of the overhead sky during a lightning storm with specific attention to the wavelength region near 450 nm that primarily contains NO_2 absorption features. Ambient NO_2 concentrations were typically less than 0.1 ppb. In the first experiment the large enhancement of over 500 percent observed in the early part of the storm was attributed to

lightning (Noxon 1976). The parcel of air with the high NO_2 concentration was assumed to be travelling with a storm cell in which the lightning flash rate of 5 per minute persisted for one hour. A NO_2 production rate of $10^{26} \text{ NO}_2/\text{flash}$, certain to within one order of magnitude, was derived from the overhead column.

It was not possible to determine how much of the measured NO_2 was in the clouds overhead where the absorption signal could be greatly enhanced by multiple scattering. A second set of experiments in which stormy areas were observed horizontally below the level of the clouds resolved this difficulty (Noxon 1978). Table 3 shows a data summary for experiments under various lightning conditions. The results confirm that 10^{26} NO_2 molecules are created per flash beneath the clouds. Observations of the sky where only corona discharges were occurring showed NO_2 concentrations comparable to the typical ambient values, indicating that they were a minimal source of NO_2 during thunderstorms. An in-situ measurement such as this avoids many of the large uncertainties associated with lightning discussed in the previous section as well as some uncertainties in the rainout process discussed in Chapter IV. Noxon's (1976;1978) value of 10^{26} NO_2 molecules produced per flash from cloud-to-ground will be used for further calculations in this work. In order to properly evaluate this recommendation, a more detailed discussion of the experimental uncertainties follows.

Although NO is initially created in a lightning discharge, Noxon's measurement of NO_2 approximates the NO_x produced, since under dark sky conditions prevalent during a thunderstorm most of the NO is rapidly converted to NO_2 by reaction with ozone. In full daylight the NO_2 is photolyzed to NO; a photochemical steady state exists and NO and NO_2 rapidly cycle among themselves. Immediately after a sudden decrease in solar intensity, such as in an eclipse, the cycling ceases and NO_2 builds up on the order of a few minutes in the troposphere. The rate at

which this build-up occurs is limited by the ambient ozone concentration and the rate of mixing of the lightning channel air with the ambient surroundings. The most serious uncertainty inherent in Noxon's measurements is the possibility that the NO₂ may have been entrained from the stratosphere where higher mixing ratios of NO₂ exist as the result of the strong updrafts that occur during thunderstorms. In order to address some of these questions, in-situ NO₂ measurements both below and within the clouds are needed.

Table 3. NO₂ PRODUCED BY LIGHTNING

Date	Conditions	NO ₂ Abundance ppb
Fritz Peak		
July 1975	zenith cloud, 4 flash/min	100
July 1976	zenith cloud, 1 flash/min	25,<3*
July 10, 1976	zenith cloud, 1 flash/min	20,<3*
July 18, 1976	at 4-km distant sunlit peak	2
July 21, 1976	zenith cloud after 3 strokes	10,<2†
July 23, 1976	sunlit peak, 1 flash/5 min	3
July 31, 1976	sunlit peak, 1 flash/min	10
Langmuir Laboratory		
Aug. 19, 1976	sunlit horizon sky, 3 flash/min	50
Aug. 21, 1976	sunlit horizon sky, 3 flash/min	30
Aug. 23, 1976	sunlit horizon sky, corona, no lightning	<0.3
Aug. 26, 1976	sunlit horizon sky, corona, no lightning	<0.1
<small>* 1 hour later. † 1 hour earlier.</small>		
<small>Source: Noxon (1978)</small>		

D. PREVIOUS ESTIMATES FOR GLOBAL NO_x

Table 4 lists the assumptions that have been made by previous workers about lightning parameters to obtain the global NO_x production rates given in Table 2. The accumulation of uncertainties can readily be seen in the range of various parameters, especially when they are combined to give the global average of the total energy dissipated in J/cm²s.

The annual number of lightning flashes to ground that occur worldwide is generally given as 100/s and is the value adopted by all of the works listed in Table 4. Although this estimate is based on weak historical evidence of visual counting, more recent measurements do not seriously contradict it. The review by Orville and Spencer (1979) indicates that the values show a seasonal dependence and that the average appears to be less by about a factor of two. Comparisons among the different estimates for NO_x production must be done carefully since not all the estimates include a contribution from intracloud discharges. The globally integrated rate of intracloud discharges is generally quoted as 300-400 flashes/s (Uman 1969; Chalmers 1967). It must be recognized that experimental data about intracloud discharges is generally obtained from indirect means such as surface electric field, electric field charge, and thunder measurements; therefore the experimental uncertainties are quite large. Also the body of information about intracloud discharges is smaller and more recent than the more easily studied ground-stroke phenomenon. More about the lightning parameters and their uncertainties will be said in Chapter 3, where the global distribution data used in this study are discussed.

TABLE 4. SUMMARY OF LIGHTNING FLASH DATA USED FOR GLOBAL
 NO_x ESTIMATES

Energy Deposited J/m	Stroke Length km	Strokes per Flash	Flashes per Second	Total Energy Dissipated J/cm ² s	References
10^5	6.25	1	100 CG a 400 IC	6.2×10^{-8}	Tuck 1976
10^5	5	4	100 CG b 300 IC	1.6×10^{-7}	Chameides et al. 1977
10^5	5	4	100 CG b 300 IC	1.6×10^{-7}	Chameides 1979
10^4	5	1.5	100 CG c	1.5×10^{-9}	Hill 1980
10^4	10	1.0	100 CG a 400 IC	1.0×10^{-8}	Dawson 1980
-	-	-	-	10^{-8}	Levine et al. 1981

CG = Cloud-to-ground. IC = Intracloud.

a. Uman 1969

b. Chalmers 1967

c. Turman 1978; Orville and Spencer 1979.

III. GLOBAL DISTRIBUTION OF LIGHTNING AND NO_x

A. GLOBAL LIGHTNING

So far the approach taken has been to adopt Noxon's (1976) in-situ measurement for NO_x/flash. Lightning count data and global lightning distributions are required next. Most recent global distribution data are obtained from satellites which measure either the direct flash rate with visible or near IR sensors or an indirect quantity which can be related to flash rate, as is done with measurements of radio frequency emission. The detection threshold of the optical counting sensors needs to be high to eliminate as much noise as possible, so that only the most energetic lightning flashes are recorded. In both types of measurements a normalization to an absolute flash rate is necessary.

1. Local Flash Rate

The recent review by Orville and Spencer (1979) discusses a set of electric field lightning experiments over Jacksonville, Florida on July 22, 1974 for which DMSP satellite data was recorded 20 minutes later. The local flashing rate obtained on the ground of approximately 1 s^{-1} compares reasonably well with the local rate of 0.4 s^{-1} estimated from the satellite if one assumes that the characteristics of the storm did not change much in the intervening time.

Electric field measurements by Livingston and Krider (1978) have been used to normalize the most recently reported DMSP satellite data by Turman and Edgar (1980). The ground measurements from June 1 to July 15, 1975 were combined with the ground measurements of Jacobson and Krider (1976) between June 15 and July 30, 1974. In a 300-km² experimental area at the

Kennedy Space Center, about 38 percent of the lightning flashes were to ground and the total lightning density to ground was about 6 flashes/km²/month.

The use of local flash rate data to normalize satellite data brings to mind several difficulties. If the identical storm is not observed by both systems, sufficient data averaging must be done to incorporate the natural variations. The detection systems used are generally not the same; for the two examples discussed here, electric field measurements were done on the ground and optical sensors were used from the satellite. The detection efficiencies may vary for ground flashes and most probably do vary for cloud-to-ground vs. intracloud flashes.

2. Intracloud vs Cloud-to-Ground Lightning

An experimental determination of the ratio of the number of intracloud discharges to the cloud-to-ground strokes, N_c/N_g , requires counting both lightning events with equal efficiency. In practice, this is difficult to do since the ease of counting cloud-to-ground strokes tends to bias the ratio to values which are too low. Accurate lightning counting of intracloud discharges by optical means is very difficult. First of all, in many cases the visibility within a cloud is too poor to permit identification of a lightning event. Also, precipitation below the clouds diminishes the visibility even further. At long distances, discharges within the clouds often cannot be distinguished from ground flashes.

Various indirect methods have been used to distinguish between the two forms of lightning. Radio noise emitted from lightning discharges can be used to selectively detect either cloud-to-ground strokes or intracloud discharges, depending on the frequency region monitored. Table 5 shows that emission from the ground stroke predominates at lower frequencies and at higher frequencies, above about 1 MHz, both emit with equal intensity. At still higher frequencies, greater

than about 10 MHz, Kreielsheimer and Lodge-Osborn (1971) found that gaps in the radiative noise from the two types of lightning followed different distribution laws which could be used to selectively choose between them. Ground-based measurements can make use of the entire frequency range, but measurements from satellites must be done in frequency regions that exceed the critical frequency of the ionosphere. Electric field change measurements can also be used to distinguish between the two types of lightning by the different features present in the electric field change time record. A more detailed discussion of the experimental methods used to determine the ratio N_c/N_g is presented by Prentice (1977).

TABLE 5. RADIO FREQUENCY EMISSION FROM CLOUD AND GROUND STROKES

Frequency	Amplitude Ratio (ground stroke/cloud stroke)
3 kHz	20/1 to 40/1
6 kHz	10/1 to 20/1
10 kHz	10/1
20 kHz	5/1
30 kHz	2/1 to 3/1
50 to 100 kHz	1/1 to 1.5/1
1.5 to 12 MHz	1/1

Source: Golde 1977, p. 223.

Prentice and Mackerras (1977) have analyzed 29 data sets from 13 countries and obtained the following relationship, which generalizes the ratio N_c/N_g in a typical thunderstorm,

$$\frac{N_c}{N_g} = (4.16 + 2.16 \cos 3\lambda) \left[0.6 + \frac{0.4T}{72 - 0.98\lambda} \right] \quad (3.1)$$

where

$T \leq 84$, thunderdays per year

$\lambda \leq 60^\circ$, latitude in Northern and Southern Hemispheres.

The authors recommend equation 3.1, but if data for both the annual number of thunderdays and the latitude are unknown, the following relationships can be used to estimate the ratio N_c/N_g from either the annual thunderdays or the latitude.

$$\frac{N_c}{N_g} = 1.0 + 0.063 T, \quad (10 \leq T \leq 84) \quad (3.2)$$

$$\frac{N_c}{N_g} = 4.16 + 2.16 \cos 3\lambda, \quad (0 \leq \lambda \leq 60^\circ) \quad (3.3)$$

The ratio as a function of latitude from equation 3.3 is shown in Figure 1. This ratio has the highest value in the tropics, where most lightning activity occurs.

The partitioning between intracloud discharges and cloud-to-ground lightning can be expressed in fractional form as follows:

$$f_g = \frac{N_g}{N_g + N_c} = \frac{1}{N_c/N_g + 1} \quad (3.4)$$

$$f_c = \frac{N_c}{N_g + N_c} = \frac{N_c/N_g}{N_c/N_g + 1} \quad (3.5)$$

The amount of NO_x formed by intracloud discharges and cloud-to-ground strokes can be estimated from the energy released by intracloud lightning processes and cloud-to-ground lightning processes. The energy of a cloud-to-ground stroke can be represented by $E = 1/2 QU$ where Q is the charge transferred and U is the electrostatic potential. It is not possible to estimate the potential of a thundercloud with respect to ground because the charge distribution within a cloud is unknown; however, it is possible to estimate the potential of the upper end of the leader and ground before it reaches the earth. In a recent review by Berger (1977), typical values were 8 coulombs for the charge and 60 V/cm for the gradient along the leader which becomes 30 MV for a 5-km stroke. The voltage from the accompanying corona shell was added, resulting in a total voltage of about 50 MV. Berger concluded that a typical cloud-

to-ground stroke deposited 2×10^8 joules of energy along the lightning channel.

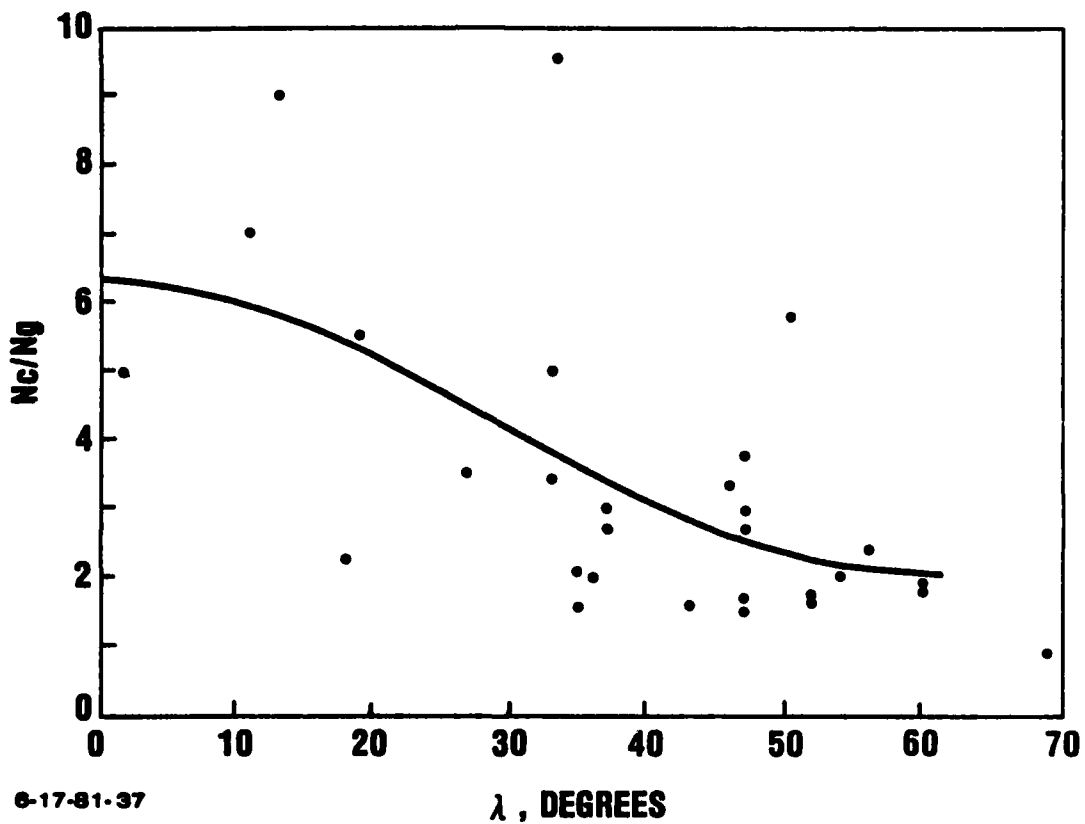


FIGURE 1. Relation between observed values of the ratio, N_c/N_g of cloud flashes to ground flashes and latitude, λ . The 29 data points and the empirical relation $N_c/N_g = 4.16 + 2.16 \cos 3\lambda$ are shown.

A similar analysis can be done for the K change stage of an intracloud discharge which is analogous to the return stroke. The review by Brook and Ogawa (1977) lists a range of dissipated charge of 10 to 100 coulombs with a typical value of about 50 coulombs. A typical discharge length was 2 km and an average electric field change upon discharge was 100 V/m. If one assumes a simple dipole interaction for the discharge process,

the energy deposited by intracloud discharges is at least one order of magnitude less than the typical cloud-to-ground stroke. It should be noted that the electric field change measurements may be indicative of charge neutralization, but it can also be caused by charge rearrangement within the cloud. Typical current estimates also support the values estimated for the deposited energy; the current dissipated by a typical intracloud discharge was estimated by Brook and Ogawa (1977) to be 1400 amperes whereas the current of a cloud-to-ground stroke is typically ten times larger. Both the potential and current arguments suggest that cloud-to-ground strokes are about ten times more energetic than cloud discharges.

Holmes et al. (1971) reviewed several experimental determinations of acoustic energy released by intracloud and cloud-to-ground lightning. Integrated thunder power spectra indicated that intracloud discharges are one third as energetic as ground flashes.

There is a large uncertainty in all the estimates of lightning energy release. The deposition of energy into air is generally inferred from indirect evidence and is difficult to estimate without ambiguity since the exact mechanism of energy deposition is not currently understood. For example, the theory of the frequency of spectrum of thunder is still a matter of controversy, so that the use of integrated power spectra to estimate the energy release is uncertain. These problems are extensively discussed in Hill's (1979) survey of lightning energy estimates.

In this report, cloud-to-ground strokes will be considered to be ten times more efficient as NO_x producers than intracloud discharges since we assume that cloud-to-ground strokes deposit ten times more energy per stroke on the average. If Holmes' factor of 3 were used instead, the results would show higher NO_x values at higher altitudes, but the total NO_x production would only increase about 50 percent, well within the estimated uncertainty.

3. Global distribution of Lightning

There are a number of measurements of the global distribution of lightning:

- (1) Optical observations of lightning flashes from the various DMSP satellite experiments by Orville and Spencer (1979) and Turman and Edgar (1980) - see Figure 2.
- (2) Observations of HF radio noise from the ISS-b satellite [Kotaki et al. (1981)] - see Figure 3.
- (3) Observations of high frequency radio noise from the ground by Davies (1965) - see Figure 4., also Crichlow et al. (1971).
- (4) Surface estimates of thunderstorm days compiled in the Handbook of Geophysics (1966) - see Figure 5.

Overall, these results seem to be fairly consistent, except for the absolute variation by a factor of 3 between items 1 and 2. The strengths and weaknesses of the data sets are listed in Table 6.

The following general characteristics are apparent:

- o Lightning occurs predominantly over or near land, at low or middle "meteorological" latitudes [namely, the latitudes relative to the Inter-Tropical Convergence Zone (ITCZ), whose mean position is at 5-10°N geographic latitude year-round, but with relatively large seasonal (Monsoonal) excursions, especially over the Indian Ocean]. There are very few thunderclouds at high latitudes because solar forcing is very weak there, nor over the open ocean where the surface is so uniform that few large disturbances are likely to be launched up to become cumulonimbus clouds.
- o A longitudinal summation of Turman and Edgar's (1980) DMSP data is shown by the bar graphs in Figure 6. It clearly shows that at dusk most of the lightning activity

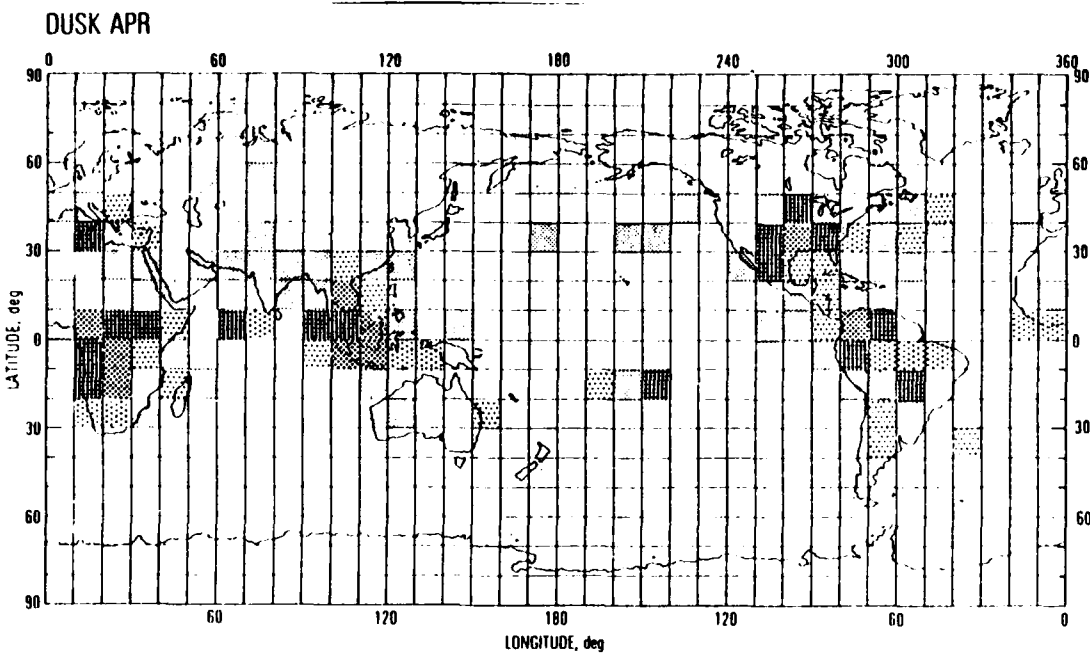


FIGURE 2. Optical observation of lightning rate from DMSP satellite for dusk in April. (Turman and Edgar 1980)

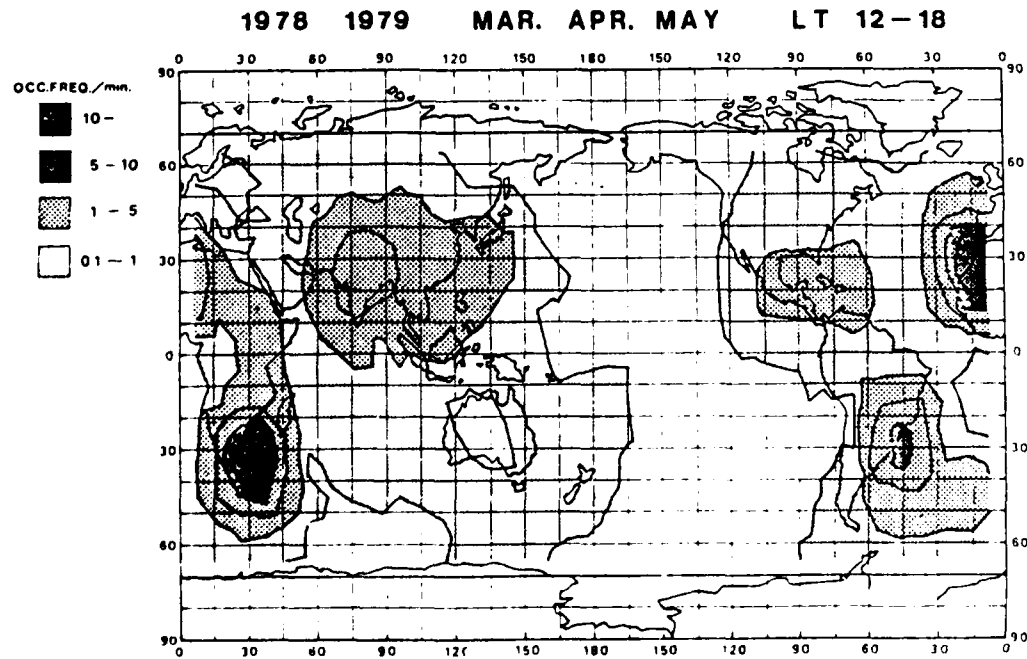


FIGURE 3. Lightning rate data from the HF radio noise data obtained by the ISS-b satellite for spring in the late afternoon and evening (Kotaki et al. 1981)

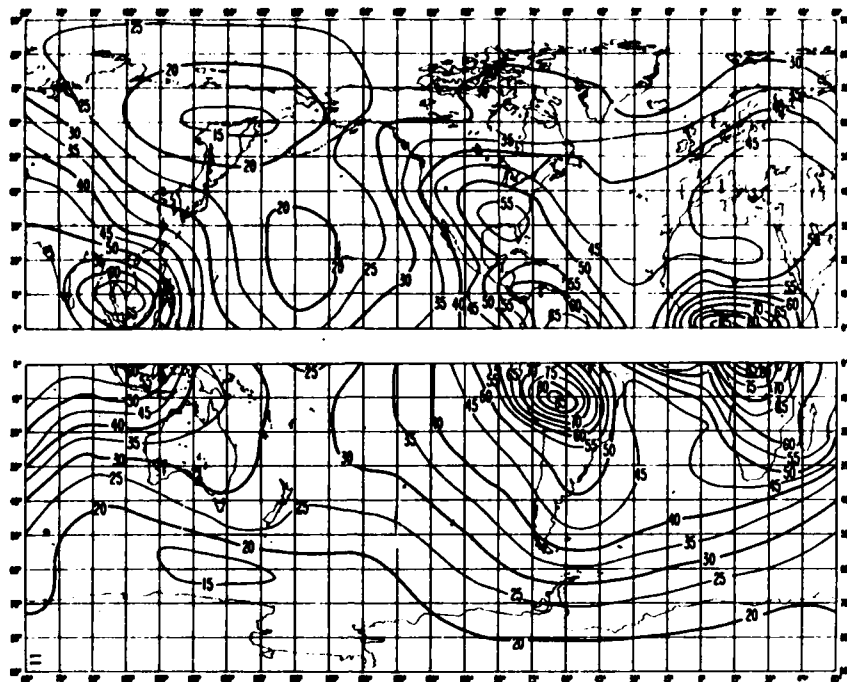


FIGURE 4. Global distribution of atmospheric radio noise obtained from ground monitoring stations. Spring season, 1200-1600 hours (CCIR Report 322 1963)

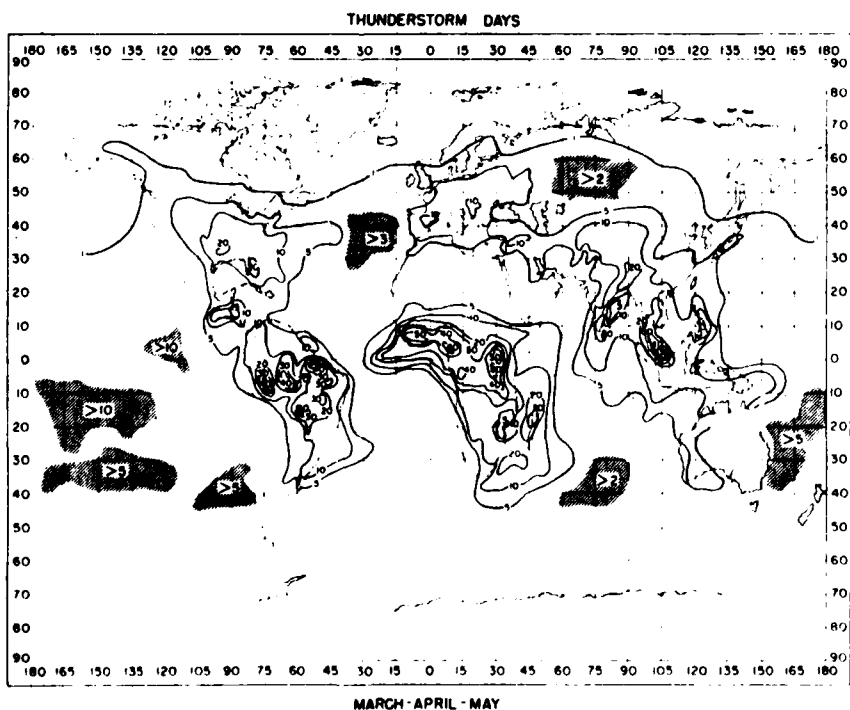


FIGURE 5. Springtime global distributions determined from ground-based observations of thunderstorms (Handbook of Geophysics 1960).

TABLE 6. STRENGTHS AND WEAKNESSES OF THE PRIMARY DATA SETS

Data Set	Strengths	Weaknesses
DMSP	<p>Satellite provides good global coverage.</p> <p>A flash is a good direct indicator.</p>	<p>Data only at dawn and dusk.</p> <p>Calibration: what is flash threshold?</p>
ISS-b	<p>Satellite provides good global coverage.</p> <p>Radio noise penetrates clouds, so in-cloud flashes are counted.</p> <p>Pulse analysis made possible direct counting of lightning events.</p>	<p>Calibration: the factor of three between DMSP and ISS-b needs to be reconciled.</p> <p>Possible interferences.</p>
HF Radio Noise	Long-term data base.	<p>Ground based: sparse global coverage-- 16 stations.</p> <p>Calibration: quantitative relationship between radio noise intensity and the lightning rate is unknown.</p>
Thunderstorm Day	Long-term data base.	<p>Ground-based, i.e., not very uniform coverage.</p> <p>Calibration: what is the relation between thunderstorm day and lightning flash rate?</p>

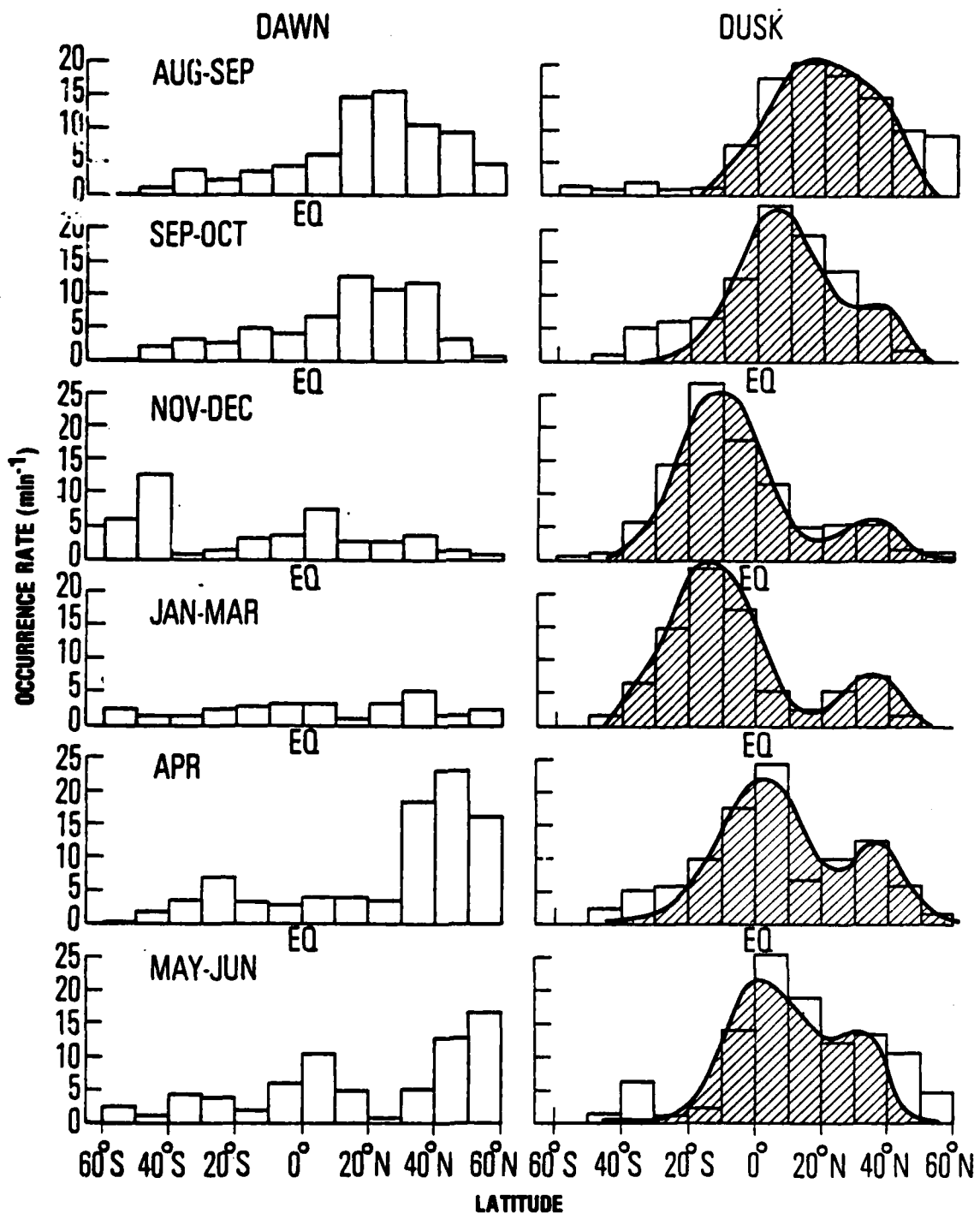


FIGURE 6. Latitudinal and seasonal dependence of the lightning rate observed from the DMSP satellite. (Turman and Edgar 1980). The curve shown for the dusk data was calculated by equation 3.6.

occurs within the latitude range ± 30 . Seasonal excursions of peak lightning activity into the midlatitudes occurs during the local summer, as one would expect.

- On a diurnal basis the frequency of lightning tends to peak in the late afternoon.

A simple gaussian analysis of the seasonal and latitudinal behavior is given by the solid curve in Figure 6 and the resulting mathematical expression for lightning flash rate in flashes per second is,

$$L(\lambda, M) = \frac{L}{1.1 \times 10^4} \left[\left(\frac{96 - \lambda_0}{4} \right) e^{-(\lambda - \lambda_0)^2 / 288} + (10 + 4A) e^{-(\lambda - 35)^2 / 128} \right] \quad (3.6)$$

where

$$\lambda = 16 \cos [30(M-7)]$$

$$A = \cos [30(M-6)]$$

λ_0 = latitude, include negative sign for Southern Hemisphere

M = month number, i.e., Jan = 1, Feb = 2, etc.

L = lightning rate, annual average in flashes/s.

It shows a small peak around 35°N latitude corresponding to lightning off the eastern coasts of the Southern U.S. and Japan that persists during all seasons. During the Northern Hemisphere summer the larger peak is predominantly caused by lightning activity over North America and the Indian Ocean area, whereas, during the Southern Hemisphere summer the peak lightning activity occurs in Brazil and the southern half of Africa.

Table 7 summarizes the latitudinal and monthly behavior of the lightning rate calculated from equation 3.6. It should be noted that equation 3.6 merely partitions the total lightning rate among the months of the year and latitudes between $\pm 60^{\circ}$, so that this treatment is valid for any global lightning rate. A value of 300 flashes/s, including both intracloud discharges and cloud-to-ground flashes, has been assumed.

TABLE 7. LIGHTNING FLASH RATE, LATITUDINAL AND SEASONAL DISTRIBUTION*

Month, M	L(λ, M), flashes/second												Global Average	Seasonal Averages		
	Jan	Feb	Mar	Apr	May	Jun	Jul	Aug	Sep	Oct	Nov	Dec				
Jan	0.6	5.4	26.6	67.2	88.3	60.3	21.4	5.1	10.2	20.0	10.3	7.3	322.7	Winter		
Feb	0.3	3.5	19.6	57.1	86.3	67.8	27.7	7.3	12.6	24.4	12.6	1.6	320.8	321.0		
Mar	0.1	0.9	7.3	31.3	69.4	80.0	48.0	16.7	17.4	30.7	15.7	2.0	319.5			
Apr	4	-	0.1	1.3	9.5	35.7	69.5	70.3	39.1	28.1	38.0	19.0	2.4	313.0	spring	
May	5	-	-	0.2	1.9	12.0	39.4	67.4	62.2	47.7	47.6	22.0	2.6	303.2		
Jun	6	-	-	-	0.4	4.1	19.8	49.8	67.3	64.8	58.1	24.8	3.1	292.2		
Jul	7	-	-	-	0.2	2.6	14.6	42.1	65.4	69.2	60.8	25.3	3.2	283.4	summer	
Aug	8	-	-	-	0.4	4.1	19.8	49.8	66.9	61.8	52.0	21.7	2.7	279.2		
Sep	9	-	-	-	0.2	1.9	12.0	39.4	67.3	61.5	42.5	37.1	16.5	2.1	280.5	
Oct	10	-	0.1	1.3	9.5	35.7	69.5	70.3	38.4	22.1	25.8	12.7	1.6	287.0	fall	
Nov	11	0.1	0.9	7.3	31.3	69.4	80.0	48.0	16.1	12.2	20.1	10.3	1.3	297.0		
Dec	12	0.3	3.5	19.6	57.1	86.3	67.8	27.7	6.9	9.7	18.3	9.4	1.2	307.8		
Annual average	0.1	1.2	6.9	22.3	42.2	52.3	49.1	37.7	33.2	36.1	16.7	2.1	300.0			
	-60	-50	-40	-30	-20	-10	0	10	20	30	40	50	60		Latitude, λ	

*An average global flash rate of 300 flashes/second has been assumed. The values listed have been calculated for each degree of latitude and summed over 10-degree latitude bins.

4. Globally Integrated Lightning Rate

Globally integrated rates of lightning observed by various satellite experiments are summarized in Table 8. Differences among the experiments can be expected, since some experiments were done at dawn and dusk and others at midnight. Most strikingly, the only experiment not done with an optical sensor records about three times more lightning than the previous works (Kotaki et al. 1981).

The geographical distribution for the ISS-b and the most recent DMSP experiment are similar (see Figures 2 and 3). It is possible that the difference in the flashing rate results from the method used to calibrate the satellite data. The following discussion summarizes the experimental techniques and calibration methods used to obtain an absolute value for the lightning flash rate.

The high-frequency radio noise observed by the ISS-b satellite (Kotaki et al. 1981) which was attributed to lightning was found to coincide with the presence of cumulonimbus clouds observed at the same time by the geostationary meteorological satellite GMS. Radio noise data was collected at 2.5, 5, 10, and 25 MHz. The frequencies were chosen to be high enough to be above the critical frequency of the ionosphere yet low enough to take advantage of the greater signal strengths. At the same time, it was necessary to avoid interference from radio transmitters.

The noise patterns were distinctive and were easily distinguished from cosmic radio noise which appeared as a constant background level and from solar radio noise originating from solar bursts which appeared as a sinusoidal signal synchronized with the spin of the satellite. About 30 percent of the time, interference from transmitters on the ground was evident but its characteristic random noise pattern, which persists over long periods of time, could be readily distinguished from the intermittent waveforms characteristic of the noise from lightning.

TABLE 8. LIGHTNING FLASHES COUNTED BY SATELLITE

Satellite	Time	Location	Flash Rate or Density	Reference
OSO-2	midnight	between 30°N and 30°S	NH = 16/s SH = 12/s	Vorpahl (1967) Vorpahl et al. (1970)
OSO-5	midnight	-	confirmed above values	Sparrow and Ney (1971)
DMSP	11/14/1972 0627 GMT	West Coast of Florida squall	0.01 flashes/km ² s	Orville and Vonnegut (1974) corrected by Croft (1977)
DMSP	4/14/1974 0554 GMT	Southeastern U.S., tornadoes	0.03 flashes/km ² s	Orville and Vonnegut (1974) corrected by Croft (1977)
DMSP	3/1974-2/1975 midnight and dusk	between 60°N and 60°S	dusk ave.=96/s midnight ave.=123/s	Orville and Spencer (1979)
DMSP-SSL	9/1974-3/1975	15 orbits	<u>6x10⁻⁸ flashes/km²s</u>	Turman 1978
	midnight only	24 storms	<u>global average</u> 31/s	
DMSP-PBE	8/1977-6/1978 dawn and dusk	global average	40-120/s*	Turman and Edgar 1980
ISS-b	4/1978-3/1980 24-hr coverage	global average	280/s	Kotaki et al. 1981

* Assumes $f_C = 628$, $f_g = 388$.

OSO = Orbiting Satellite Observatory; DMSP = Defense Meteorological Satellite Program;

ISS = Ionospheric Sounding Satellite.

Times during which interference was evident were disregarded. Digital counts were obtained when the analog signal received by the satellite detector exceeded a threshold level and had the correct waveform. A lightning event was said to occur if digital counts were observed in all the frequency channels which exceeded the critical frequency of the ionosphere simultaneously. This is a direct digital counting method that does not rely on a calibration for the absolute lightning flash rate.

The DMSP satellite measurements by Turman and Edgar (1980) were done optically with a silicon photodiode with a response function between 500 and 1100 nm. The sensor was operated in a triggered mode where only the high-frequency, high-intensity pulses were recorded in order to discriminate against interfering light sources from the earth. The result was that only the most energetic lightning strokes were observed, creating a selective discrimination against the less energetic intracloud lightning. A calibration was necessary to obtain an absolute value for the lightning rate.

Based on the results of Forrest (1950), Turman and Edgar (1980) assumed that the mean diurnal flash rate is equivalent to the instantaneous rate at dusk. Normalization for the DMSP satellite data was obtained by comparison with the ground-based electric field measurements of Livingston and Krider (1978; also see Section III.A.1) and with various other local determinations of absolute flash frequency to ground (Wanasalyja 1979; Prentice 1977). The total lightning flash rate was inferred from Livingston and Krider's (1978) measurements for Eastern Florida in which about 38 percent of the lightning flashes were striking ground. An examination of Figure 1 shows that in tropical regions, where most lightning occurs, the ratio N_c/N_g is generally higher.

If one uses an intracloud to cloud-to-ground ratio ranging between 4 and 6 to renormalize the DMSP data for latitudes between 30°N and 30°S , about 250 ± 50 flashes/s result. This

then agrees more closely with the ISS-b satellite measurement of about 280 flashes/s. In this work a rounded value of 300 flashes/s was adopted for the globally integrated lightning rate.

B. INJECTION HEIGHT OF NO_x

The discussion of injection height can be conceptually considered in two domains, first the altitude of the NO_x production and second the altitude at which the NO_x is eventually deposited, which may be different due to the violent updrafts and downdrafts associated with thunderstorms. Updrafts of 60 m/s in the center of the thunderstorm cloud surrounded by downdrafts of 35 m/s have been observed. Also, clouds rise buoyantly, causing a net transport of air.

For cloud-to-ground flashes, the initial production altitude is between the lower portion of the cloud and the ground. The thickness and altitude of thunderclouds vary greatly, but lightning rarely occurs in clouds less than 3 km thick and most lightning activity occurs in large convective storms which can extend up to 20 km in altitude. Some mean estimates of production height are listed in Table 9, but this does not directly answer the question of effective injection height, which depends on the cloud stabilization height rather than on the height of the lightning discharges.

For strong midlatitude thunderstorms it is well known that the anvil top of the cumulonimbus cloud penetrates into the stratosphere and the extent of penetration has been related to the kinetic energy associated with updrafts within a thundercloud (Vonnegut and Moore 1958). Penetrations as much as 6 km have been reported for large thunderstorms over Oklahoma (Roach 1967). The consequences of cloud-top penetration is still a matter of controversy. For example, it is not clear whether cloud-top penetration ultimately results in injection or removal of chemical species such as water vapor or ozone from

TABLE 9. SOME REPRESENTATIVE HEIGHTS OF CLOUD DISCHARGES

Height Range	Location	Reference
5.8 to 4.7	Albuquerque, NM	Workman and Holzer (1942)
5.8 to 5.2	Albuquerque, NM	Workman et al. (1942)
5.5 to 5.1	Socorro, NM	Reynolds and Neill (1955)
>8	South Africa	Malan (1956)
10 to 6	-	Hatakeyama (1958)
6	-	Tamura et al. (1958)
7 - 11 ^a	-	Takagi (1961)
3 - 6 ^b		
8.2 to 4.8	Tropics	Wang (1963)
6.0 to 4.0	Socorro, NM	Ogawa and Brook (1964)
4 to 12 ^a	Brisbane, Australia	Mackerras (1968)
1 to 8 ^b		
8	-	Nakano (1973)
5 + 1	Socorro, NM Tucson, AZ Roswell, NM Houston, TX	Teer and Few (1974)

^ahigh altitude intracloud discharges
^btypical intracloud discharges

Source: Adapted from Brook and Ogawa (1977).

the stratosphere (Barrett et al. 1972; Johnston and Solomon 1979). Stratospheric water vapor concentrations near the tropopause that are not entirely consistent with those one would expect from the Hadley cell global circulation model also indicate that the understanding of the mechanism of water vapor transfer across the tropopause is currently incomplete (Ellsaesser et al. 1980). The fate of NO₂ near the tropopause is linked to the general mass transfer behavior but not necessarily to the behavior of water vapor, which may be unique due to the existence of both liquid and vapor phases under atmospheric conditions. If the net result of a large thunderstorm is injection of tropospheric gases into the stratosphere, lightning would be a source term for the stratospheric NO_x budget and, conversely, if the net result is freeze-out and entrainment from the stratosphere, lightning would represent a stratospheric NO_x sink.

Even less information is available for tropical thunderstorms. Cloud tops as high as 20 km have been reported in both the tropics and at midlatitudes, yet these values are exceptional. In this work we shall assume that updrafts will carry chemical species to the cloud tops and that the cloud tops follow the height of the local tropopause. The following injection heights have been assumed:

Tropical injections, between $\pm 30^\circ$ latitude

intracloud	10 to 15 km
cloud-to-ground	0 to 10 km

Midlatitude injections, between $\pm (30 \text{ to } 60)^\circ$ latitude

intracloud	7 to 12 km
cloud-to-ground	0 to 7 km

The vertical distribution within the two discharge regions for each latitude interval depends on the initial vertical distribution formed by the lightning process and ultimately on the turbulent mixing that occurs during the thunderstorm.

Equilibrium calculations at elevated atmospheric temperatures show an equivalent (1 to 2 percent) mole fraction of NO below 3000 K for all tropospheric air densities (Gilmore 1974; Zinn and Sutherland 1975). This indicates a NO yield proportional to the local density or P/T. This physical picture is consistent with a density-weighted vertical distribution for the NO_x produced by lightning, assuming no other sources or sinks on this time scale.

There is little experimental verification of this point; to date all laboratory simulations of lightning-type discharges in air have been done at one atmosphere pressure. Previous photographic evidence of the lightning return stroke does indicate somewhat more luminosity near the ground, but the effect is not very marked and is difficult to quantify since some intensity reduction with height can be expected from the branching evident in the return stroke. Very recent return stroke luminosity measurements by Master et al. (1981) indicate that the current dissipation is greatest near the ground and drops off with height more rapidly than was previously suspected (Uman, private communication). The analysis of this data is still in progress, thus the effect is not yet quantified, but it is clear that a density weighting is conservative.

In this work, density-weighted injection rates were proposed for direct use in a 2-D atmospheric model. The values listed in Table S-2 in the Executive Summary were calculated from the column rates in Table 10 using atmospheric densities from the 1976 U.S. Standard Atmosphere, included on the right side of Table S-2.

Additional measurements of cloud tops are necessary to reduce the uncertainty in injection height estimates and to elucidate the mechanism of tropopause penetration. A possible way to establish the variation of cloud tops with latitude is to use stereoscopic viewing of the overlap region between the two U.S. GOES geostationary satellites (W. Shenk, private communication).

TABLE 10. SUMMARY OF LIGHTNING PARAMETERS AND NO_x INJECTION RATE.

										Global Sum			
zonal area x 10 ⁷ km ²	2.56	3.15	3.65	4.03	4.29	4.43	4.43	4.29	4.03	3.65	3.15	2.56	
Annual average lightning rate, flashes/s	0.1	1.2	6.9	22.3	42.2	52.3	49.1	37.7	33.2	36.1	16.7	2.1	
Lightning fraction, interannual, f ₁ climat., f ₂ , climat., f ₃	0.67	0.72	0.78	0.83	0.85	0.86	0.85	0.86	0.83	0.78	0.72	0.67	
NO _x (ppbv), (10 ¹²) injection rate, 10 ¹² mol/s	0.01	0.01	0.04	0.14	0.27	0.33	0.31	0.23	0.21	0.21	0.08	0.01	
NO _x (ppbv), 10 ¹² mol/s	0.00	0.03	0.11	0.28	0.48	0.54	0.52	0.42	0.42	0.59	0.35	0.05	
NO _x (ppbv), 10 ¹² mol/s	0.01	0.04	0.14	0.42	0.75	0.87	0.83	0.65	0.63	0.80	0.43	0.06	
	-60	-50	-40	-30	-20	-10	0	10	20	30	40	50	60
	LATITUDE												

C. RECOMMENDED TREATMENT OF LIGHTNING AND NO_x DISTRIBUTIONS

How should the global distribution data be modelled? For convenience, a summary of the recommended values needed to calculate the global distribution is included in Table 10. The ratio N_c/N_g has been calculated from equation 3.3 and the fractions of lightning to ground and within the clouds, f_g and f_c were calculated for 10-degree latitude intervals using equations 3.4 and 3.5. NO_x production by a intracloud discharge has been assumed to be one tenth as efficient as a cloud-to-ground stroke based on the discharge energy considerations discussed in Section III.A.2.

The total NO_x injection rate in grams of nitrogen per year can be calculated for each latitude and month as follows:

$$R(\lambda, M)_c = f_c \cdot L(\lambda, M) \cdot 0.1C \quad (3.7)$$

$$R(\lambda, M)_g = f_g \cdot L(\lambda, M) \cdot C \quad (3.8)$$

where

$$C = \left(\frac{10^{26} \text{ NO}_2}{\text{flash}} \right) \cdot \left(\frac{\text{mole}}{6.02 \times 10^{23} \text{ NO}_2} \right) \cdot \left(\frac{14 \text{ gN}}{\text{mole}} \right) \cdot \left(\frac{3.2 \times 10^7 \text{ s}}{\text{yr}} \right)$$

and L(λ, M) is the lightning rate calculated from equation 3.6. The annual average injection rate is 1.85 Tg N/yr for intra-cloud discharges and 3.82 Tg N/yr for cloud-to-ground strokes. A depth of 5 km was chosen for the region where the NO_x had been deposited by intracloud discharges and the maximum altitude of this region was chosen to model the annual average tropopause height. Figure 7 shows the vertical and latitudinal distribution of NO_x production for the intracloud and cloud-to-ground regions. An atmospheric density-weighted partitioning with altitude for each region is suggested. Values for a 2-D NO_x distribution are listed in Table S-2 of the Executive Summary.

For a 3-D distribution the reader is referred directly to the DMSP satellite maps which contain latitudinal and longitudinal lightning rate distributions.

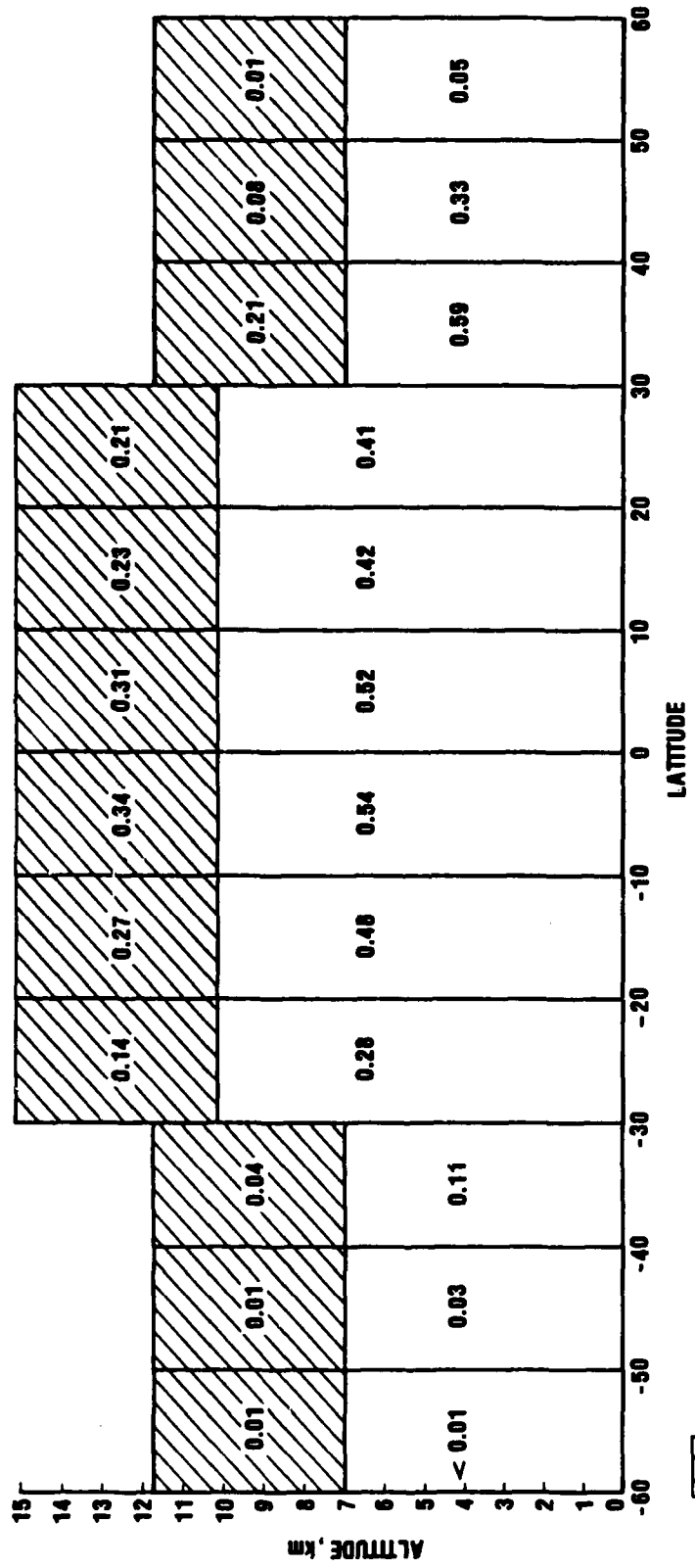


FIGURE 7. 2-D NO_x distribution in 10¹² gN/yr injected into the troposphere by lightning

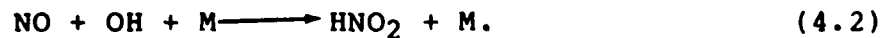
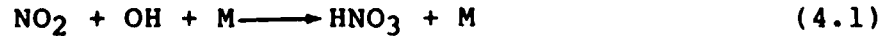
The user should distribute the values in each discharge region over the desired number of altitude bins. A density-weighted distribution with a 1-km altitude spacing is given on page S-6. For an alternate latitudinal spacing, the user is referred to the text.

IV. RAINOUT OF NO_x PRODUCED BY LIGHTNING

Historically, the search for experimental evidence of NO_x production by a lightning flash has been approached by looking for enhancement of the local HNO₃ concentration in rainwater collected on the ground which was correlated with the number of flashes or the intensity of flashes. To date, no such enhancement has been documented (e.g., Viemeister 1960; Visser 1961; Reiter 1970). A positive correlation has been found between the NO₃⁻ concentration dissolved in rainwater and both in-cloud turbulence and the time integral of electrical field strength (Reiter 1970 and references cited therein). The NO_x formation was attributed to corona discharges during the thunderstorm. Experiments of this type are difficult to extrapolate to gas phase NO_x concentrations in the troposphere since dissolved NO₃⁻ is the result of homogeneous and heterogeneous chemical reactions that are not well understood, especially under thunderstorm conditions.

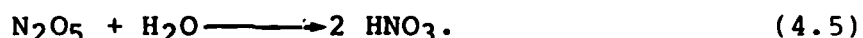
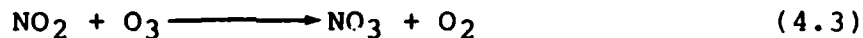
Loss mechanisms for NO₂ formed by a lightning flash during a thunderstorm include the following:

- Gas phase reactions among NO_x species that produce HNO₃ or HNO₂ during the initial stages after the lightning flash when high temperatures and high local NO_x concentrations are present.
- The gas phase reactions to form nitric and nitrous acids



This proceeds best in the presence of sunlight when higher OH concentrations are present.

- The gas phase reaction sequence,



This sequence proceeds best in the absence of sunlight, when photolysis of NO_2 , NO_3 , and N_2O_5 is slow.

- The dry deposition of gas or particles.
- Heterogeneous reaction on particles or water droplets.

The lifetime of NO_2 with respect to each of these processes is listed separately in Table 11. Since the mean lifetime of a cumulonimbus cloud is about 30 minutes, it is evident that none of these mechanisms is an important loss term.

TABLE 11. APPROXIMATE LIFETIME FOR INDIVIDUAL NO_2 LOSS MECHANISMS

Loss Mechanism	NO_2 Lifetime	Condition for Validity
$\text{NO}_2 + \text{OH} + \text{M} \xrightarrow{k_1} \text{HNO}_3 + \text{M}$	3 - 17 hrs	With daytime ambient $[\text{OH}] = (1-6) \times 10^6 \text{ cm}^{-3}$
	10 hrs	In absence of sunlight
$\text{NO}_2 + \text{O}_3 \longrightarrow \text{NO}_3 + \text{O}_2$ $\text{NO}_3 + \text{NO}_2 \longrightarrow \text{N}_2\text{O}_5$ $\text{N}_2\text{O}_5 + \text{H}_2\text{O} \xrightarrow{k_4} 2 \text{ HNO}_3$	50 - 500 hrs	In absence of sunlight $[\text{H}_2\text{O}] = 3 \times 10^{16} \text{ cm}^{-3}$
Dry deposition $\text{NO}_2 \longrightarrow \text{ground}$	1 - 10 days	Probably closer to 1 day within the planetary boundary layer.
Heterogeneous reaction on particles or water droplets	*	

*Dissolution of gaseous NO_2 and NO into water is minimal. The Henry's Law Coefficients are 1.2×10^{-2} and 6×10^{-3} M/atm, respectively. Heterogeneous reaction rates on particles depend on the local aerosol concentration levels which vary widely.

$k_1 [\text{M}] = 1.6 \times 10^{-11} \text{ cm}^3 \text{ molec}^{-1} \text{ s}^{-1}$
 $k_4 < 10^{-20} \text{ cm}^3 \text{ molec}^{-1} \text{ s}^{-1}$

A. NO_x LOSS

1. NO_x Loss: HNO₃ Formation in High Local NO_x Air

Immediately after the lightning flash it is possible for chemical conversion of NO_x to HNO₃ to occur readily because of the locally high NO concentrations. When the air in the lightning channel has reached the NO freeze-out temperature, the local NO mole fraction can be as high as 1 to 5 percent. Under such conditions, homogeneous and heterogeneous reactions such as



as well as reaction sequence 4.3 to 4.5 can be extremely fast. As the lightning channel continues to expand and mix with the surrounding air, the temperature approaches ambient and the NO_x concentration approaches the parts per billion range. At complete dilution the rate of reaction among the NO_x reactants becomes extremely slow.

Another mechanism for nitrous and nitric acid formation has been proposed by the time-and-temperature dependent, chemical kinetic, hot-channel-model calculations of Hill and Rinker (1981) which focused on the production of HNO₃ and HNO₂ within the heated air produced by lightning. The 24 chemical species created by lightning from N₂, O₂, H₂O, and CO₂ were assumed to be in thermodynamic equilibrium by the time the hot channel of air had expanded and cooled to 3000 K. The calculated time and temperature dependence of HNO₂ and HNO₃ formation as the gases cooled, expanded, and mixed with the surrounding air showed an increased production that was not simply fixation of products formed at higher temperatures. HNO₂ and HNO₃ formation by reactions 4.1 and 4.2 represent loss terms for the NO, NO₂ and OH concentrations which are maintained by thermal equilibrium, and

thus a net production of nitrogen species occurs even below the temperature of NO concentration freeze-out. The amount of nitrate formation, $1.6 \times 10^{15} \text{ NO}_3^-$ per cm^3 of heated lightning channel air at 3000 K, was consistent with the 0.2 ppm NO_3^- observed in rainfall at sea by Gambell and Fisher (1964), assuming that all the HNO_3 and HNO_2 formed in the heated channel rained out. For extremely soluble species such as nitric and nitrous acids, this is a reasonable assumption.

The remaining NO is chemically converted to NO_2 , primarily by the reactions



where RO_2 is HO_2 , CH_3O_2 and higher organic peroxy radials. The chemical conversion occurs in 2 to 6 minutes for temperatures between 300 and 240 K or altitudes between 0 and 10 km. At somewhat higher temperatures, before the mixing and dilution is complete, the conversion occurs at a faster rate. During the daytime, photochemical steady state exists for NO and NO_2 . The NO lost chemically by reactions 4.9 and 4.10 is rapidly regenerated by NO_2 photolysis which in turn regenerates ozone



Logan et al. (1981) show the diurnal variation of NO_x and HO_x calculated with a 1-D model for the tropics (15° N) and midlatitudes (45° N) at heights of 0 and 6 km. The ground level midlatitude results reproduced in Figure 8 show that both the NO_x and HO_x chemical systems respond immediately to the sudden solar intensity changes at sunrise and sunset. Clean air measurements at Niwot Ridge, CO, have shown NO_2/NO ratios of 100 ppt/20 ppt in the morning and 300 ppt/50 ppt in the

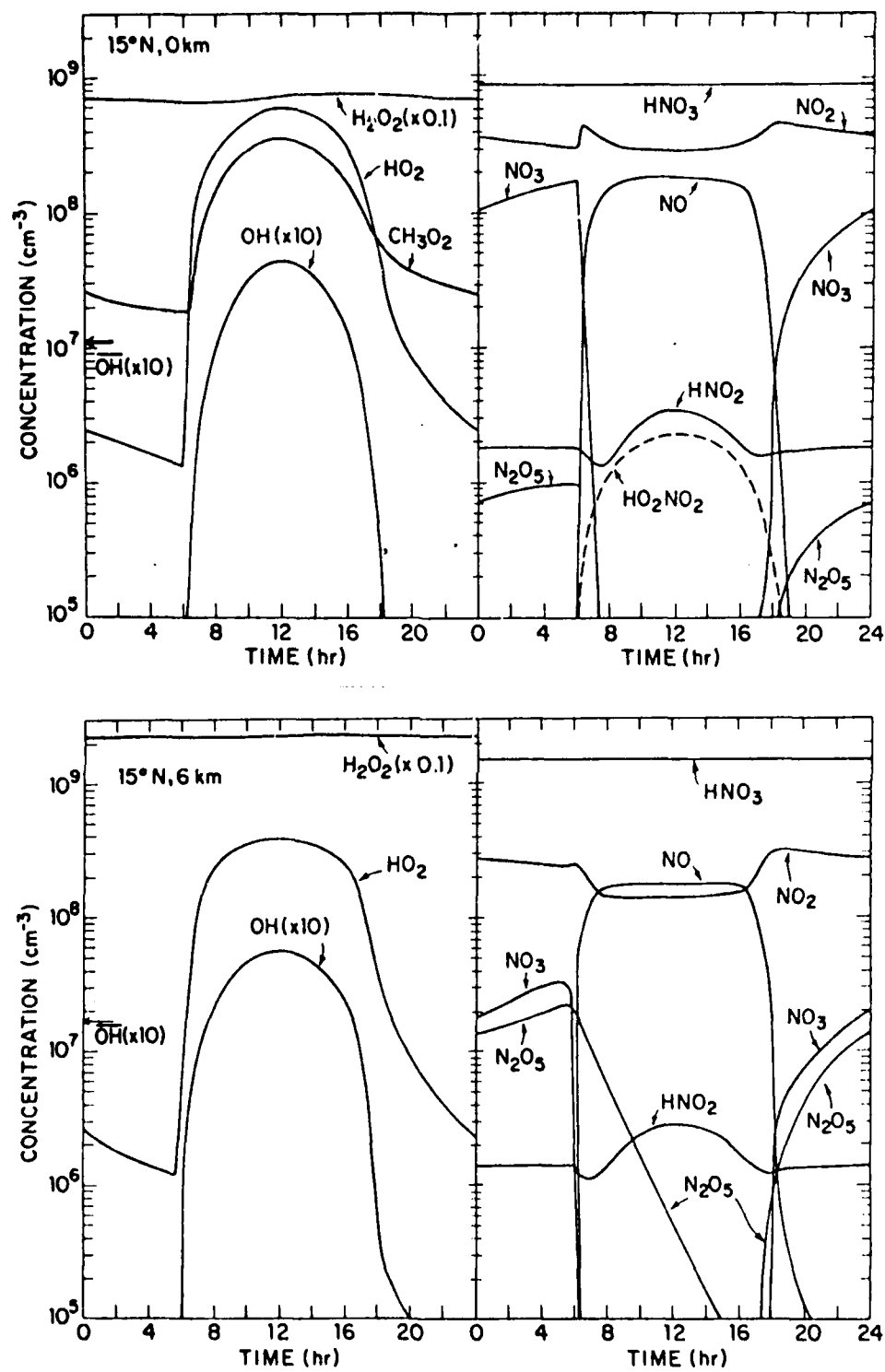


FIGURE 8. Diurnal behavior of the NO_x AND HO_x chemical systems in the troposphere at 15° N latitude equinox, calculated with 1-D model. The upper set of figures is for ground level conditions; the lower set is for an altitude of 6 km.

Source: Logan et al. 1981.

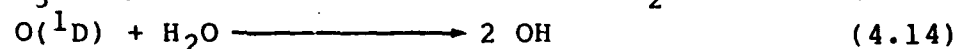
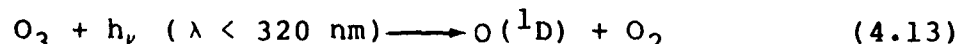
late afternoon (Kelly et al. 1980). The rate of oxidation of NO to NO₂, and thus the ratio of NO₂/NO, depends on the local NO, O₃ and organic peroxy radical concentrations, the temperature, the sunlight intensity, as well as any local turbulence which disperses the NO_x. A large injection of NO can deplete the local O₃ concentration, slowing the conversion time of NO to NO₂ to several hours (Jordan and Broderick 1979). About 70 percent of the solar radiation in the visible wavelength region, where NO₂ absorbs strongly, is reflected by dense cloud tops. During a thunderstorm, turbulence increases the oxidation rate to NO₂ and the dark overhead sky reduces the NO₂ photolysis rate, so that the NO₂ concentration can build up.

Noxon's (1976) measurement of NO₂ produced by lightning can be considered a lower-limit estimate of the actual NO_x produced, since total conversion to NO₂ was assumed and no conversion to HNO₃ was considered. The NO_x that is immediately converted to HNO₃ after the lightning flash and is rained out, is lost to the atmospheric NO_x inventory. It is not necessary to estimate this quantity since we are concerned with gas phase NO_x produced by lightning that can remain after the thunderstorm to add to the tropospheric NO_x inventory. Any losses of NO_x that occur during the thunderstorm but after Noxon's measurements do represent losses that need to be estimated.

2. NO_x Loss: HNO₃ Formation by NO₂ + OH + M

To determine the efficiency of the gas phase reaction that produces HNO₃ it is necessary to estimate the OH concentration. Experiments by Campbell et al. (1979), in which chemical oxidation of radioactively labeled CO were used, indicate that under daytime conditions the OH concentration can vary between 3×10^5 to $3 \times 10^6 \text{ cm}^{-3}$ in the unpolluted tropospheric boundary layer. Tropospheric measurements by Wang and Davis (1974), Wang et al. (1975), and Davis et al. (1976, 1979) using laser fluorescence indicate OH concentrations that are an order of magnitude higher, but it is possible that an experimental artifact caused unnaturally high values to be measured (Ortgies et al. 1980).

Most tropospheric OH is initially produced by the mechanism



so that one can expect a variation in solar intensity to produce a variation in OH concentration (Levy II, 1972). This is corroborated by the ozone photodissociation constant measurements by Dickerson et al. (1979) (see Figure 9). The variation of $O(^1D)$ production with solar zenith angle was what one would expect from atmospheric path length considerations. Superimposed on the data were rapid spikes which corresponded to, at most, a 50 percent reduction in $O(^1D)$ production caused by passing clouds. The UV intensity that produces the residual $O(^1D)$ is most likely due to scattering from the blue sky surrounding the cloud. An experiment in which the solar disk was blocked out but the remaining daylight was allowed to enter the reaction vessel supported this hypothesis (Dickerson 1980).

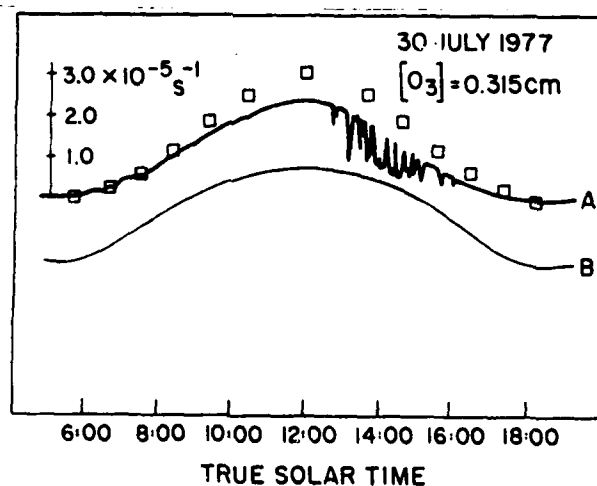
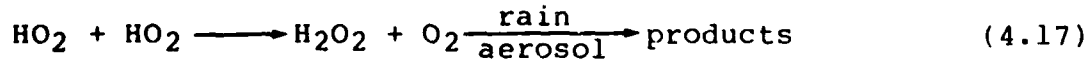
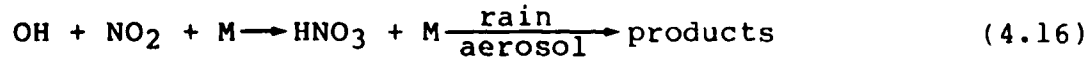


FIGURE 9. Curve A, Data for $O_3 + h\nu \longrightarrow O(^1D) + O_2$ photodissociation constant, showing the effect of passing clouds. \square was calculated using atmospheric absorption and Rayleigh scattering. Curve B is $\exp(-1/\cos \theta)$.

Source: Dickerson et al. 1979.

In order to make estimates for the OH concentration that exists during a thunderstorm, one needs to consider the amount of light that produces O(¹D), i.e., the 295-320 nm wavelength region, that can reach a parcel of air under the thundercloud. The optical density for UV and near-UV radiation is sufficiently high within the cloud so that the cloud can be considered opaque. Scattering from the surrounding sky to the parcel of air underneath the cloud can be considered negligible, since most thunderclouds hang low near the ground and extend far vertically, i.e., the base of a cumulonimbus cloud is typically 0-3 km above the ground, and the vertical extent is 5 km. Direct illumination beneath the cloud for the maximum 3 km height cloud is only possible for zenith angles greater than 40°, which occurs at local solar times between 3 p.m. and sunset. Thunderstorms generally occur in the late afternoon when the O(¹D) production rate is rapidly decreasing, i.e., during the summer at 3 p.m. solar time the O(¹D) production rate was lower by 60 percent when compared to the noontime value (see Figure 9). The loss of the photolytic source for OH in most of the troposphere during a thunderstorm results in an extremely low OH concentration if the chemical sources are small.

During the daytime the rate of interconversion of OH and HO₂ is exceedingly fast so that the chemical lifetime of OH is dominated by the reactions that determine the chemical lifetime of HO_x. The photolysis reaction sequence 4.13 - 4.14 is the main source of tropospheric HO_x. The sinks of HO_x are radical termination reactions such as



There are many chemical reactions or reaction sequences that cycle HO_x; for example, the reactions of OH with O₃, CO, CH₄, and H₂O₂ and the reactions of HO₂ with O₃ and NO. These processes establish a steady-state concentration of OH on the order of 10⁵ to 10⁶ molecules/cm³.

The daylight ambient concentrations of HO₂ and NO₂ are generally about 100 times greater than OH and assure that the OH is rapidly removed after the photolytic source of OH ceases. In the absence of sunlight the HO_x source term vanishes but the chemical removal reactions remain operative. This implies an immediate drop in OH concentration and a slower decay of HO₂ which is verified by model calculations through a solar eclipse (Herman 1979a) and diurnal model calculations at sunset (Logan et al. 1981), an example of which is shown in Fig. 8. In a darkened sky the OH concentration is not high enough for the NO₂ + OH + M reaction to proceed at an appreciable rate during the lifetime of the thunderstorm.

3. NO_x Loss: HNO₃ Formation via N₂O₅

In the absence of sunlight, most of the atmospheric NO is converted to NO₂ and NO₃ and an equilibrium between NO₂, NO₃ and N₂O₅ is established. Experiments by Noxon et al. (1978) show that in the stratosphere this process occurs in about 40 minutes. To some extent, one would expect this to also occur in the troposphere during a thunderstorm when the overhead sky is dark. The N₂O₅ can react with water vapor, present at high concentrations during a thunderstorm, to form HNO₃. (See reactions 4.3 to 4.5.) The rate constant for N₂O₅ + H₂O is known only as an upper limit and this discussion presents the maximum possible NO₂ loss to HNO₃ via N₂O₅. A further complication exists since it is possible that this reaction is actually heterogeneous, therefore, aerosols and particulates may be necessary for HNO₃ formation.

The lifetime of NO_2 can be estimated from the ratio of NO_2 to its loss rate by this mechanism

$$\tau = \frac{[\text{NO}_2]}{k_5 [\text{N}_2\text{O}_5] [\text{H}_2\text{O}]} \quad (4.18)$$

The N_2O_5 concentration has not been measured in the troposphere but it can be inferred from NO_2 and NO_3 concentrations and the equilibrium constant which have been measured. An upper limit for the tropospheric vertical column density of NO_3 of $0.2 \times 10^{14} \text{ cm}^{-2}$ has been measured by Noxon et al. (1978). In this experiment NO_2 concentrations less than 1 ppb were required to be consistent with calculations. In a similarly clean atmosphere Noxon (1978) measured NO_2 column densities of 10^{15} cm^{-2} in the troposphere, which corresponds to 0.2 ppbv at the surface. The equilibrium constant for reaction 4.4 shows an extreme temperature dependence, i.e., the calculated N_2O_5 concentration increases by a factor of 10 for a 20-degree temperature decrease of 320 to 300 K (Connell and Johnston 1979). For this same temperature range the water vapor pressure drops by a factor of 3. With a typical midlatitude water vapor content during a storm of about $3 \times 10^{16} \text{ molecules/cm}^3$ the lifetime from equation 4.18 is about 500 hrs at 300 K. Using the most extreme water vapor content recorded at ground level for the tropical regions of $3 \times 10^{17} \text{ molecules/cm}^3$ reduces all the lifetime estimates by a factor of 10. At minimum tropospheric temperatures, i.e., between 10 to 20 km, N_2O_5 production becomes more favorable; however, the H_2O vapor concentration is lower by four orders of magnitude. The resulting removal of NO_2 via N_2O_5 is minimal high in the troposphere if the N_2O_5 concentration has not increased more than 3 orders of magnitude. Such an increase is unlikely, since the local NO_2 concentration sets an upper limit on the N_2O_5 concentration present at low temperatures. Also, the arguments which depend on an equilibrium between N_2O_5 , NO_2 , and NO_3 are uncertain since one cannot assume

an equilibrium exists in the cold troposphere where the rate of thermal decomposition of N_2O_5 is very slow.

The best estimate that can be made for the conversion of NO_2 to HNO_3 in the absence of sunlight is that this conversion is minimal throughout the troposphere during the lifetime of a thunderstorm, but it is difficult to quantify it more exactly. It should be possible to make a better assessment when the tropospheric N_2O_5 concentration has been measured directly. Conclusions based on NO_3 and NO_2 data alone are difficult to use due to the sensitivity of the NO , NO_2 , NO_3 , and N_2O_5 chemical system to the vertical temperature profile.

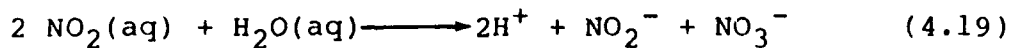
4. NO_x Loss: Dry Deposition

The fourth mechanism for the loss of NO and NO_2 created by lightning is dry deposition onto ground or water surfaces. The deposition velocity which is used to quantify the rate of mass transfer from the gas phase to the surface is typically between 0.1 and 1 cm/s at a reference height of 1 km or at the top of the logarithmic wind profile within the planetary boundary layer. The value of the deposition velocity depends on a number of factors; for example, the altitude, the exact nature of the interaction of the molecule with the surface, the temperature, the wind speed, etc. The following deposition velocities for species of interest in the NO_x chemical system have been recently measured over a grassland: $\text{HNO}_3 = 0.34 \pm 0.25$, $\text{O}_3 = 0.67 \pm 0.15$, $\text{NO}_x = 0.73 \pm 0.24$ cm/s at a reference height of 1 m (Kasting, 1980). For a 1-km mixing height of the daytime boundary layer, a range for the deposition velocity of 0.1 to 1 cm/s results in a deposition rate of 10^{-5} to 10^{-6} seconds⁻¹ or a 1/e lifetime between 1-10 days. For a chemical species as reactive as NO_2 , the faster deposition rate is probably more appropriate.

5. NO_x Loss: Aerosol Scavenging and Rainout

The final mechanism for loss of NO_2 is heterogeneous reactions on particles or water droplets. It is unlikely that

significant amounts of gaseous NO_2 will dissolve into water droplets to be rained out during the lifetime of the thunder-storm, since the various factors governing the solubility of gaseous NO_2 are unfavorable. Dissolution involves three equilibrium processes: (1) partitioning between the gaseous and aqueous phases which is parameterized by the Henry's Law coefficient, (2) an aqueous phase equilibrium of the NO_2 to form chemically associated oxyacids such as HNO_2 and HNO_3 , and (3) an acid dissociation equilibrium in which the ionic species H^+ , NO_2^- or NO_3^- are formed. The equilibrium concentration calculated by Henry's Law indicates that the gaseous NO_2 can enter the liquid phase to form a 0.007 molar solution per atmosphere NO_2 (Lee and Schwartz 1981a). Partitioning into the atmosphere is favored; the NO_2 experiences liquid phase resistance to mass transfer (Eisenreich et al. 1981). The extent to which the NO_2 forms dissociated acid within the liquid depends on the kinetics of the following reaction.



Lee and Schwartz's (1981a) recent kinetic study, done with NO_2 partial pressures comparable to those found in the polluted troposphere, showed that the time constant for the above reaction is at least ten times slower than the time for convective or diffusive mass transport within the liquid. This indicates that NO_2 dissolution is limited by both the rate of physical transfer from the gas phase to the aqueous phase and by the rate of ion formation in solution to a sufficient extent so that very little of the NO_2 produced during the lightning storm is immediately dissolved and rained out.

Recently an experimental study was presented in which the chemistry of NO_2 with realistically simulated clouds was studied. (Miller and Gertler 1981). For 0.1 ppm NO_2 in clean air, the rate of conversion to NO_3^- in the cloud was 0.04 percent/hr. This corresponds to a lifetime of 1700 hrs for NO_2 .

It is also possible that the dissolution of NO_2 may be aided by the presence of oxidizing or reducing agents present in the rain droplets or on the surface of particles. Although heterogeneous chemistry is not well understood, some progress has been made by the environmental requirement to remove NO_x from power plant and industrial plant effluents. Most NO_x removal schemes include the use of a catalyst or a chemical reaction sequence which first oxidizes or reduces the NO_x to enhance the solubility into the liquid phase where it is eventually converted to a gas or to an insoluble solid which precipitates (Faucett 1977). Studies by Lee and Schwartz (1981b) indicate that the uptake of NO_2 by liquid water is potentially important for catalyst concentrations on the order of 10^{-7} M and a fast rate constant for reaction 4.19. They found that the Fe catalyzed reaction is not important but the reaction of NO_2 with dissolved S(IV) is potentially important. It is difficult to estimate to what extent such heterogeneous chemistry enhances the dissolution of NO_2 into raindrops in the troposphere, since the concentration of catalysts and other dissolved species in raindrops is uncertain.

B. HNO_3 LOSS: RAINOUT, DRY DEPOSITION AND HETEROGENEOUS SCAVENGING

The small amount of the gaseous HNO_3 that is formed during the lightning storm, as well as the residual HNO_3 formed before the storm, is quickly rained out. Table 12 summarizes the partitioning between gaseous and aqueous HNO_3 calculated from equilibrium considerations. The aqueous phase is strongly favored. Table 13 shows that the scavenging coefficient for HNO_3 into cumulus clouds is fast enough that within a cloud, gaseous HNO_3 is quickly dissolved within water droplets (Levine and Schwartz 1981). The scavenging coefficients for a heavy rainfall are also fast enough that any residual HNO_3 vapor is quickly picked up by the falling water droplets and rained out.

TABLE 12. EQUILIBRIUM OF HNO_3 WITH WATER*

P_{HNO_3} (atm)	$[\text{HNO}_3]_g^{**}$ mol cm^{-3}	$[\text{HNO}_3]_{\text{aq}}/[\text{HNO}_3]_g$
10^{-8}	2.6×10^{11}	50
10^{-10}	2.6×10^9	500

Source: Levine and Schwartz 1981.

*The water vapor content assumed is 10^{-6} g cm^{-3} .

**Note that the measured $[\text{HNO}_3]_g$ in the troposphere range from 0.1 - 5 ppb (2.6×10^9 - 1.3×10^{11} mol cm^{-3}) (Kelley et al. 1979).

TABLE 13. HNO_3 SCAVENGING BY CLOUDS AND RAINFALL

Scavenging Medium	Scavenging Coefficient	Scavenging Time
Cumulus clouds	0.2 s^{-1}	5 seconds
Light rain 1 mm hr^{-1}	$1.3 \times 10^{-5} \text{ s}^{-1}$	21 hours
Heavy rain 25 mm hr^{-1}	$1.5 \times 10^{-3} \text{ s}^{-1}$	11 minutes
Long-term average: includes rain and dry deposition.	$(1-8) \times 10^{-6} \text{ s}^{-1}$	1 - 11 days
Aerosol Scavenging by Rainfall		
Medium rain $10 - 18 \text{ mm hr}^{-1}$	$1 - 3.3 \times 10^{-3} \text{ s}^{-1}$	5 - 15 minutes

Source: HNO_3 data compiled from Levine and Schwartz 1981.
Aerosol data from Radke et al. 1980.

The importance of heterogeneous rainout was shown by a tropospheric modelling calculation for HNO_3 by Fishman and Crutzen (1977). An order of magnitude decrease in tropospheric HNO_3 concentration was noted when a heterogeneous removal process with a rate of $2 \times 10^{-6} \text{ s}^{-1}$ was added for the lowest 6 km. The calculation by Levine and Schwartz (1981) shows that the long-term average for scavenging by falling raindrops and dry deposition is $(1 \text{ to } 8) \times 10^{-6} \text{ s}^{-1}$.

In a heavy rainstorm the scavenging efficiency of gaseous HNO_3 by falling raindrops and the scavenging efficiency of aerosol particles by rain are comparable. This is shown in Table 13. In addition, if one assumes that deposition of HNO_3 onto atmospheric aerosol particles occurs at the same rate as dry deposition to the ground, the removal of HNO_3 vapor by aerosols is very effective.

Overall, the removal of HNO_3 by various heterogeneous processes is very efficient. This is what one would expect since 20 to 40 percent of the acid content in rain over polluted areas is HNO_3 (Likens et al. 1979). Also, measurements of the HNO_3 content in air before and after rainfall shows that rainfall is a very effective removal process. Previous workers have tried to correlate the HNO_3 measured in rain with lightning activity with no success (Viemeister 1960; Visser 1960; Reiter 1970). This is what one would expect if the NO_x produced by lightning is not converted to HNO_3 during the lifetime of the thunderstorm.

V. UNCERTAINTIES AND RECOMMENDATIONS

A. UNCERTAINTIES

There are several major sources of uncertainty apparent in the estimate of the lightning contribution to the global NO_x budget:

- The NO_x production efficiency for both cloud-to-ground lightning and intracloud discharges.
- The injection height of NO_x produced during a lightning storm, and its vertical distribution.
- The normalization of the global lightning rate measured by satellite, especially in the tropics.
- The ratio of cloud discharges to ground flashes, also with particular emphasis in the tropics.

Noxon (1976, 1978) estimated the uncertainty of the NO_2 production rate to be within one order of magnitude. This does not include the systematic error, if any, introduced by extrapolating Noxon's midlatitude measurement to the tropics, and by assuming that the NO_2 measured by Noxon is equivalent to NO_x .

It should be emphasized here that in some cases assumptions have been made because direct experimental evidence does not exist. For example, the estimate of NO_x production by intracloud discharges has been based on the argument that the amount of NO_x produced is directly proportional to the discharge energy and that, on the average, cloud discharges are about one tenth as energetic as the ground flash. The mean stroke length for intracloud and cloud-to-ground lightning was assumed to be equivalent. Even though some exceptionally long intercloud discharges have been observed, e.g., 50 km, much cloud lightning is of the shorter, intracloud type. The maximum height of NO_x injection

was assumed to follow the height of local tropopause, but again, no experimental evidence exists to support this conclusion.

A large uncertainty is introduced by current normalization techniques employed for satellite experiments. Simultaneous satellite and ground-based measurements provide good calibration points, provided that some tropical as well as midlatitude coverage is included. For accurate global counting, the efficiency of intracloud detection needs to be carefully considered, since certain satellite and ground-based techniques selectively discriminate against the less energetic events such as intracloud discharges.

Another uncertainty is introduced through the large scatter of the N_c/N_g ratio evident in Figure 1. In part, this is due to an inadequate statistical sample and in part to natural variations over different geographical terrain. The deficiency can be remedied with more satellite experiments properly equipped with sensors equally sensitive to cloud discharges and ground flashes. Special attention should be given to the tropical regions where current data is sparse but where most of the lightning activity occurs.

The overall uncertainty has been estimated to be approximately one order of magnitude, reflecting the accumulation of uncertainty in the measured quantities only. For quantities where no measurements exist, such as the NO_x production efficiency by cloud discharges and the injection height, it is not possible to estimate the uncertainty.

B. RECOMMENDATIONS

Most of the uncertainties mentioned can be resolved using previously developed experimental systems. For example, a set of experiments capable of measuring in-situ NO_x at various altitudes during a thunderstorm could eliminate the uncertainty of the injection height and the uncertainty of the NO_x production efficiency by cloud discharges. Similar experiments are

routinely made for environmental monitoring of NO_x in ambient air at ground level. The NO concentration has been measured from an aircraft during the GAMETAG experiments (Davis 1980) and NO and NO_2 have been measured several times in balloons (see for example McFarland et al. 1979).

The following recommendations are made here:

- The F-106B aircraft used in the NASA Langley Storm Hazard Project, which is currently equipped to fly within thunderstorms, could be easily adapted to accommodate an NO_x monitoring system. Several measurements should be made at various altitudes within the thundercloud, at its perimeter, and outside the cloud in order to sample regions of net updrafts and downdrafts. This single experiment would answer both the question of NO_x production efficiency by cloud discharges as well as the net injection height during and after the thunderstorm. A global aircraft study is not needed at this time; global behavior could be inferred from other parameters.
- The NO_x measurements, such as Noxon's column densities, are needed in the tropics to determine whether the production efficiency by lightning is different for tropical thunderstorms.
- Experimental observation of lightning by satellite presents a comprehensive and consistent global distribution, but a consensus for the globally averaged lightning rate does not exist. The problem of calibration of the satellite lightning measurements should be specifically addressed. Satellite experiments should be combined with ground-based measurements to provide an absolute calibration for the flash rate in both the tropics and the midlatitudes. Preferably, experimental systems capable of detecting both cloud discharges and ground flashes should be chosen.

- Several measurements of the ratio of cloud discharges to ground flashes are needed in the tropics to reduce the scatter evident in currently available data. In general, tropical regions are poorly represented by individual experimental measurements, but it should be recognized that most lightning occurs there.

An experiment in which all NO_y species, i.e., NO , NO_2 , HNO_3 , HNO_2 , and possibly NH_3 and NO_3 , will be measured simultaneously during a thunderstorm is currently being prepared at the Georgia Institute of Technology (M. O. Rodgers, private communication). The concentrations will be monitored in a parcel of air before, during, and after a thunderstorm, using laser-induced fluorescence combined with photofragmentation techniques when necessary (Rodgers et al. 1980). Although this experimental system cannot be routinely employed or placed in an aircraft because it is too expensive, bulky, and heavy, several individual experiments would answer questions about chemical production efficiencies by lightning, the partitioning among the NO_y species in the thunderstorm environment, and the effectiveness of rainout for the various chemical species. The direct concentration measurements to be obtained from this experiment complement Noxon's measurements of the NO_2 column density.

REFERENCE LIST

Barrett, E.W., P.M. Kuhn, and A. Shlanta, Recent Measurements of the Injection of Water Vapor and Ozone Into the Stratosphere by Thunderstorms, Second Conference on CIAP, A.J. Broderick, ed., Report DOT-TSC-OST-73-4, pp. 34-46, 1972.

Bauer, E., Natural and Anthropogenic Sources of Oxides of Nitrogen (NO_x) for the Troposphere, IDA Paper P-1619 (in publication), 1982.

Berger, K., "The Earth Flash," in Lightning, Volume I, Physics of Lightning, ed. by R.H. Golde, Academic Press, New York, 119-190, 1977.

Berger, K., "Methoden und Resultate der Blitz-Forschung auf dem Monte San Salvatore 1963-71," Bull. Schweiz. Elektrotech. Ver., 64, 120-136, 1972.

Brode, H.L. "Numerical Solutions of Spherical Blastwaves," J. Appl. Phys., 26, 766-775, 1955.

Brook, M. and T. Ogawa, "The Cloud Discharge," in Lightning, Volume 1, Physics of Lightning, R.H. Golde, ed., Academic Press, New York, 191-230, 1977.

Campbell, M.J., J.C. Sheppard, and B.A. Au, "Measurement of Hydroxyl Concentration in Boundary Layer Air by Monitoring CO Oxidation," Geophys. Res. Lett., 6, 175-178, 1979.

Chalmers, J.A., Atmospheric Electricity, Pergamon Press Ltd., New York, 515, 1967.

Chameides, W.L., "Effect of Variable Energy Input on Nitrogen Fixation in Instantaneous Linear Discharges," Nature, 277, 123-125, 1979.

Chameides, W.L., D.H. Stedman, R.R. Dickerson, D.W. Rusch, and R.J. Cicerone, "NO_x Production in Lightning," J. Atmos. Sci., 34, 143-149, 1977.

Connell, P. and H.S. Johnston, "The Thermal Dissociation of N₂O₅ in N₂," Geophys. Res. Lett., 6, 553-556, 1979.

Crichlow, W.Q., R.C. Davis, R.T. Disney, and M.W. Clark, Hourly Probability of World-wide Thunderstorm Occurrence, U.S. Dept. of Commerce, Office of Telecommunications, OT/ITS RR 12 (COM-75-1202), April 1971.

Croft, T.A., Nocturnal Images of the Earth From Space, Stanford Research Institute, Rep. No. 68197, 107, 1977.

Crutzen, P.J. "The Role of NO and NO₂ in the Chemistry of the Troposphere and Stratosphere," Ann. Rev. Earth and Planet. Sci., 7, 443-472, 1979.

Davis, D.D., "Project GAMETAG: An Overview," J. Geophys. Res., 85, 7285-7292, 1980.

Davis, D.D., W. Heaps, and T. McGee, "Direct Measurement of Natural Tropospheric Levels of OH via an Aircraft-Borne Tunable Dye Laser," Geophys. Res. Lett., 3, 331-333, 1976.

Davis, D.D., W. Heaps, D. Phalen, and T. McGee, "Boundary Layer Measurements of the OH Radical in the Vicinity of an Isolated Power Plant Plume: SO₂ and NO₂ Conversion Times," Atmos. Environ., 13, 1197-1203, 1979.

Davies, K., Ionospheric Radio Propagation, NBS Monograph 80, 1965. Reprinted by Dover, 1966.

Dawson, G.A. "Nitrogen Fixation by Lightning," J. Atmos. Sci., 37, 174-178, 1980.

Dickerson, R.R., Ph.D. thesis, University of Michigan, 1980.

Dickerson, R.R., D.H. Stedman, W.L. Chameides, P.J. Crutzen and J. Fishman, "Actinometric Measurements and Theoretical Calculations of $j(O_3)$, the Rate of Photolysis of Ozone to O(¹D)," Geophys. Res. Lett., 6, 833-836, 1979. Correction to this paper, 1980: Geophys. Res. Lett., 7, 112.

Eisenreich, S.J., B.B. Looney, and J.D. Thornton, "Airborne Organic Contaminants in the Great Lakes Ecosystem," Environ. Sci. Technol., 15, 30-38, 1981.

Ellaesser, H.W., J.E. Harries, D. Kley, and R. Penndorf, "Stratospheric H₂O," Planet Space Sci., 28, 827-835, 1980.

Faucett, H.L., J.D. Maxwell, and T.A. Burnett, Technical Assessment of NO_x Removal Processes for Utility Application, EPA-600/7-77-127 and EPRI AF-568, 397, 1977.

Fishman, J. and P.J. Crutzen, "A Numerical Study of Tropospheric Photochemistry Using a One-dimensional Model," J. Geophys. Res., 82, 5897-5906, 1977.

Foley, H.M. and M.A. Ruderman, "Stratospheric NO Production From Past Nuclear Explosions," J. Geophys. Res., 78, 4444-4450, 1973.

Forrest, J.S., "Variations in Thunderstorm Severity in Great Britain," Quart. J. Roy. Meteorol. Soc., 76, 277, 1950.

Gambell, A.W. and D.W. Fisher, "Occurrence of Sulfate and Nitrate in Rainfall," J. Geophys. Res., 69, 4203-4210, 1964.

Gilmore, F.R., "The Production of Nitrogen Oxides by Low-Altitude Nuclear Explosions," J. Geophys. Res., 80, 4553-4554, 1975. Also published in more detail in IDA Paper P-986, 1974.

Golde, R.H., Lightning, Volume I, Physics of Lightning, R.H. Golde, ed., Academic Press, New York, 1977.

Goldsmith, P., H.F. Tuck, J.S. Foot, E.L. Simmons, and R.L. Newson, "Nitrogen Oxides, Nuclear Weapon Testing, Concorde and Stratospheric Ozone," Nature, 244, 545-551, 1973.

Griffing, G.W., "Ozone and Oxides of Nitrogen Production During Thunderstorms," J. Geophys. Res., 82, 943-950, 1977.

Hameed, S., O.G. Paidoussis, and R.W. Stewart, "Implications of Natural Sources for the Latitudinal Gradients of NO_y in the Unpolluted Troposphere," Geophys. Res. Lett., 8, 591-594, 1981.

Hatakeyama, H., "The Distribution of the Sudden Change of Electric Field on the Earth's Surface Due to Lightning Discharge," in Recent Advances in Atmospheric Electricity, L.G. Smith, ed., Pergamon Press, London, 289-298, 1958.

Herman, J.R. "The Response of Stratospheric Constituents to a Solar Eclipse, Sunrise and Sunset," J. Geophys. Res., 84, 3701-3710, 1979a.

Herman, J.R., "The Problem of Nighttime Stratospheric NO₃," J. Geophys. Res., 84, 6336-6338, 1979b.

Hill, R.D., "A Survey of Lightning Energy Estimates," Rev. Geophys. Space Phys., 17, 155-164, 1979a.

Hill, R.D. "On the Production of Nitric Oxide by Lightning," Geophys. Res. Lett., 6, 945-947, 1979b.

Hill, R.D., "Channel Heating in Return-Stroke Lightning," J. Geophys. Res., 76, 637-645, 1971.

Hill, R.D. and R.G. Rinker, "Production of Nitrate Ions and Other Trace Species by Lightning," J. Geophys. Res., 86, 3203-3209, 1981.

Hill, R.D., R.G. Rinker, and H. Dale Wilson, "Atmospheric Nitrogen Fixation by Lightning," J. Atmos. Sci., 37, 179-192, 1980.

Holmes, C.R., M. Brook, P. Krehbeil, and R. McCrory, "On the Power Spectrum and Mechanism of Thunder," J. Geophys. Res., 76, 2106-2115, 1971.

Jacobsen, E.A. and E.P. Krider, "Electrostatic Field Changes Produced by Florida Lightning," J. Atmos. Sci., 33, 103-117, 1976.

Johnston, H.S. and S. Solomon, "Thunderstorms as a Possible Micrometeorological Sink for Stratospheric Water," J. Geophys. Res. 84, 3155-3158, 1979.

Johnston, H.S., G. Whitten, and J. Birks, "Effect of Nuclear Explosions on Stratospheric Nitric Oxide and Ozone," J. Geophys. Res., 78, 6107, 1973.

Jordan, B.C. and A.J. Broderick, "Emissions of Oxides of Nitrogen from Aircraft," J. Air Pollut. Control Assn., 29, 119-124, 1979.

Kasting, J.F., "Determination of Deposition Velocities for O₃ NO_x and HNO₃ by the Gradient Method," in The CHON Photochemistry of the Troposphere, Notes from a Colloquium: Summer 1980, National Center for Atmospheric Research, Boulder, CO, 161-172, 1980.

Kelly, T.J., D.H. Stedman, and G.L. Kok, "Measurements of H₂O₂ and HNO₃ in Rural Air," Geophys. Res. Lett., 6, 375-378, 1979.

Kelly, T.J., D.N. Stedman, J.A. Ritter, and R.B. Harvey, "Measurements of Oxides of Nitrogen and Nitric Acid in Clean Air," J. Geophys. Res. 85, 7417-7425, 1980.

Kitagawa, N., M. Brook, and E.J. Workman, "Continuing Currents in Cloud-to-Ground Lightning Discharges," J. Geophys. Res., 67, 637-647, 1962.

Kotaki, M., I. Kuriki, C. Katoh, and H. Sugiuchi, "Global Distribution of Thunderstorm Activity," Private communication, 1981. Also to be published in J. Radio Res. Labs., Japan.

Kreuelsheimer, K.S. and D. Lodge-Osborn, "New Developments in Lightning Counter Design," Proc. Inst. Elect. Engrs., 118, 79-87, 1971.

Krider, E.P., G.A. Dawson, and M.A. Uman, "Peak Power and Energy Dissipation in a Single-Stroke Lightning Flash," J. Geophys. Res., 73, 3335-3339, 1968.

Latham J. and I.M. Stromberg, "Point Discharge," in Lightning, Volume 1, Physics of Lightning, R.H. Golde, ed., Academic Press, New York, 99-117, 1977.

Lee, Y.N. and S.E. Schwartz, "Reaction Kinetics of Nitrogen Dioxide with Liquid Water of Low Partial Pressure," J. Phys. Chem., 85, 840-848, 1981a.

Lee, Y.N. and S.E. Schwartz, "Evaluation of the Rate of Uptake of Nitrogen Dioxide by Atmospheric and Surface Liquid Water," Accepted for publication in J. Geophys. Res., paper 1C7346, 1981b.

Levine, J.S., R.S. Rogowski, G.L. Gregory, W.E. Howell, J. Fishman, "Simultaneous Measurement of NO_x , NO, O_3 Production in a Laboratory Discharge: Atmospheric Implications," Geophys. Res. Lett., 8, 1981.

Levine, S.Z. and S.E. Schwartz, "In-Cloud and Below-Cloud Scavenging of Nitric Acid Vapor," 1981. Accepted for publication in Atmospheric Environment.

Levy II, H., "Photochemistry of the Lower Troposphere, Planet. Space Sci., 20, 919-935, 1972.

Likens, G.E., R.F. Wright, J.N. Galloway, and T.J. Butler, "Acid Rain," Sci. Am., 241, 43-51, 1979.

Lin, S.C., "Cylindrical Shock Waves Produced by Instantaneous Energy Release," J. Appl. Phys., 25, 54-57, 1954.

Livingston, J.M. and E.P. Krider, "Electric Fields Produced by Florida Thunderstorms," J. Geophys. Res., 83, 385-401, 1978.

Logan, J.A. M.S. Prather, S.C. Wofsy, and M.B. McElroy, "Tropospheric Chemistry: A Global Perspective," J. Geophys. Res., 86, 7210-7254, 1981.

Mackerras, D., "A Comparison of Discharge Processes in Cloud and Ground Lightning Flashes," J. Geophys. Res., 73, 1175-1183, 1968.

Malan, D.J., "Visible Electrical Discharges Inside Thunderclouds," Geofis. Pura Appl., 34, 221-236, 1956.

Malan, D.J., "The Relation Between the Number of Strokes, Stroke Intervals and the Total Duration of Lightning Discharges," Geofis. Pura Appl., 34, 224-230, 1956.

Master, M.J., M.A. Uman, Y.T. Lin and R.B. Standler, "Calculations of Lightning Return Stroke Electric and Magnetic Fields Above Ground," 1981. To appear in December 1981 J. Geophys. Res.

McFarland, M., D. Kley, J.W. Drummond, A.L. Schmeltekopf, and R.H. Winkler, "Nitric Oxide Measurements in the Equatorial Pacific Region," Geophys. Res. Lett., 6, 605-608, 1979.

Miller, D.F. and A.W. Gertler, "Acid Formation in Cloud Water as Affected by Gaseous NO₂," EOS Trans. AGU, 62, 884, 1981.

Nakano, M., "Lightning Channel Determined by Thunder," Proc. Res. Inst. Atmos., Nagoya Univ., 20, 1-7, 1973.

Noxon, J.F., Correction, J. Geophys. Res., 4560-4561, 1980.

Noxon, J.F., "Tropospheric NO₂," J. Geophys. Res., 83, 3051-3057, 1978.

Noxon, J.F., "Atmospheric Nitrogen Fixation by Lightning," Geophys. Res. Lett., 3, 463-465, 1976.

Noxon, J.F., R.B. Norton, and W.R. Henderson, "Observation of Atmospheric NO₃," Geophys. Res. Lett., 5, 675-678, 1978.

Ogawa, T. and M. Brook, "The Mechanism of the Intracloud Lightning Discharge," J. Geophys. Res., 69, 5141-5150, 1964.

Ortgies, G., K.H. Gericke, and F.J. Comes, "Is UV Laser-Induced Fluorescence a Method to Monitor Tropospheric OH?" Geophys. Res. Lett., 7, 905-908, 1980.

Orville, R.E., "A High-Speed Time-Resolved Spectroscopic Study of the Lightning Return Stroke 1, 2, 3," J. Atmos. Sci., 25, 1968.

Orville, R.E., "Ozone Production During Thunderstorms Measured by the Ultraviolet Radiation from Lightning," J. Geophys. Res., 72, 3557-3561, 1967.

Orville, R.E. and D.W. Spencer, "Global Lightning Flash Frequency," Monthly Weather Review, 107, 934-943, 1979.

Orville, R.E. and B. Vonnegut, "Lightning Detection from Satellites, Electrical Processes in Atmospheres, H. Dolezalek and R. Reiter, eds., Steinkopff Verlag, Darmstadt, 750-753, 1974.

Picone, J.M., J.P. Boris, J.R. Frieg, M. Rayleigh, and R.F. Fernsler, Convective Cooling of Lightning Channels, Naval Research Laboratory Memorandum Report 4472, 1981. Also J. Atmos. Sci., 38, 2056-2062, 1981.

Ploooster, M.N., "Numerical Model of the Return Stroke of the Lightning Channel," Phys. Fluid, 14, 2124-2133, 1971.

Prentice, S.A., "Frequencies of Lightning Discharges," in Lightning, Volume 1, Physics of Lightning, R.H. Golde, ed., Academic Press, New York, 465-496, 1977.

Prentice, S.A., and D. Mackerras, "The Ratio of Cloud to Cloud-to-Ground Lightning Flashes in Thunderstorms," J. Appl. Meteorol., 16, 545-550, 1977.

Radke, L.F., P.V. Hobbs, and M.W. Eitgroth, "Scavenging of Aerosol Particles by Precipitation," J. Appl. Meteorol., 19, 715-722, 1980.

Reiter, R., "On the Causal Relation Between Nitrogen-Oxygen Compounds in the Troposphere and Atmospheric Electricity," Tellus, 22, 122-135, 1970.

Reynolds, S.E. and H.W. Neill, "The Distribution and Discharge of Thunderstorm Charge-Centers," J. Meteorol., 12, 1-12, 1955.

Roach, W.T., "On the Nature of the Summit Areas of Severe Storms in Oklahoma," Quart. J. Roy. Meteorol. Soc., 93, 318-336, 1967.

Rodgers, M.O., K. Asai, and D.D. Davis, "Photofragmentation-Laser-Induced Fluorescence: A New Method for Detecting Atmospheric Trace Gases," Appl. Optics, 19, 3597-3605, 1980.

Salanave, L.E., "Recent Advances in the Observation of Lightning Spectra," Planetary Electrodynamics, Gordon and Breach, New York, 449-464, 1969.

Salanave, L.E., R.E. Orville, and C.N. Richards, "Slitless Spectra of Lightning in the Region from 3850 to 6900 Angstroms," J. Geophys. Res., 67, 1877-1884, 1962.

Schiff, H.I., D. Pepper, and B.A. Ridley, "Tropospheric NO Measurements up to 7 km," J. Geophys. Res., 84, 7895, 1979.

Schonland, B.F.J., "The Lightning Discharge," in Handbuch der Physik, 22, Springer-Verlag OHG, Berlin, 576-628, 1956.

Smith, L.G., "Atmospheric Electricity," in USAF Handbook of Geophysics, Revised edition, MacMillan Co., New York, Chapter 9, 1960.

Sparrow, J.G. and E.P. Ney, "Lightning Observations by Satellite," Nature, 232, 540-541, 1971.

Sparrow, J.G. and E.P. Ney, "Discrete Light Sources Observed by Satellite OSO-B," Science, 161, 459-460, 1968.

Takagi, M., "The Mechanism of Discharge in a Thundercloud," Proc. Res. Inst. Atmos., Nagoya Univ., 1-106, 1961.

Tamura, Y., T. Ogawa, and A. Okawati, "The Electrical Structure of Thunderstorms," J. Geomagn. Geoelect., 10, 20-27, 1958.

Teer, T.L. and A.A. Few, "Horizontal Lightning," J. Geophys. Res., 79, 3436-3441, 1974.

Tuck, A.F., "Production of Nitrogen Oxides by Lightning Discharges," Quart. J. Roy. Meteorol. Soc., 102, 749-755, 1976.

Turman, B.N., "Lightning Detection From Space," Am. Scientist, 67, 321-329, 1979.

Turman, B.N., "Analysis of Lightning Data From the DMSP Satellite," J. Geophys. Res., 83, 5019-5024, 1978.

Turman, B.N., "Detection of Lightning Superbolts," J. Geophys. Res., 82, 2566, 1977.

Turman, B.N. and B.C. Edgar, Global Lightning Distributions at Dawn and Dusk, The Aerospace Corporation, Space Sciences Laboratory Report No. SSL-80(5639)-1, 1980. Also to be published in J. Geophys. Res., (paper 1C1286), 1981.

Uman, M.A., Lightning, McGraw-Hill, 264, 1969.

Uman, M.A., A.H. Cookson, and J.B. Moreland, "Shock Wave From a Four-Meter Spark," J. Appl. Phys., 41, 3148-3155, 1970.

Uman, M.A., R.E. Orville, A.M. Sletten, and E.P. Krider, "Four-Meter Sparks in Air," J. Appl. Phys., 39, 5162-5168, 1968.

Viemeister, P.E., "Lightning and the Origin of Nitrates Found in Precipitation," J. Meteorol., 17, 681-683, 1960.

Visser, S., "Chemical Composition of Rain Water Found in Kampala, Uganda and Its Relation to Meteorological and Topographical Conditions," J. Geophys. Res., 66, 3759-3765, 1961.

Vonnegut, B. and C.B. Moore, "Giant Electrical Storms," in Recent Advances in Atmospheric Electricity, Permagon Press, London, 339-411, 1958.

Vorpahl, J.A., "The Frequency and Intensity of Lightning within 30° of the Equator," Masters thesis. University of Minnesota, 66, 1967.

Vorpahl, J.A., J.G. Sparrow, and E.P. Ney, "Satellite Observations of Lightning," Science, 169, 860-862, 1970.

Wallace, L., "Note on the Spectrum in the Region 3670 to 4280 Å," J. Geophys. Res., 65, 1211-1214, 1960.

Wanasalyja, O., "The Communications Industry's Requirements and Interests," Proceedings: Workshop on the Need for Lightning Observations from Space, L.S. Christensen, W. Frost, W.W. Vaughan, eds., NASA CP-2095, 1979.

Wang, C.P., "Lightning Discharges in the Tropics. 2. Component Ground Strokes and Cloud Dart Streamer Discharges," J. Geophys. Res., 68, 1951-1958, 1963.

Wang, C.C., and L.I. Davis, Jr., "Measurement of Hydroxyl Concentrations in Air Using a Tunable UV Laser Beam," Phys. Rev. Lett., 32, 349-352, 1974.

Wang, C.C., L.I. Davis, C.H. Wu, S. Japar, H. Niki, and B. Weinstock, "Hydroxyl Radical Concentrations Measured in Ambient Air," Science, 189, 797-800, 1975.

Workman, E.J. and R.E. Holzer, A Preliminary Investigation of the Electrical Structure of Thunderstorms. Tech. Notes Natn. Advis. Comm. Aeronaut. No. 850, 1942.

Workman, E.J., R.E. Holzer and G.T. Pelsor, The Electrical Structure of Thunderstorms. Tech. Notes Natn. Advis. Comm. Aeronaut. No. 864, 1942.

Zinn, J. and C.D. Sutherland, Chemical Equilibria in Hot Air with Moisture, Salt, and Vaporized Metal Contaminants, Los Alamos Scientific Laboratory Report LA-5850-MS, 1975.

END

LOVED

DID